Journal of Medicinal Chemistry

Article

pubs.acs.org/jmc

Carbamoyl Pyridone HIV-1 Integrase Inhibitors 3. A Diastereomeric Approach to Chiral Nonracemic Tricyclic Ring Systems and the Discovery of Dolutegravir (S/GSK1349572) and (S/GSK1265744)

Brian A. Johns,*[,†] Takashi Kawasuji,[‡] Jason G. Weatherhead,[†] Teruhiko Taishi,[‡] David P. Temelkoff,[†] Hiroshi Yoshida,[‡] Toshiyuki Akiyama,[‡] Yoshiyuki Taoda,[‡] Hitoshi Murai,[‡] Ryuichi Kiyama,[‡] Masahiro Fuji,[‡] Norihiko Tanimoto,[‡] Jerry Jeffrey,[†] Scott A. Foster,[†] Tomokazu Yoshinaga,[‡] Takahiro Seki,[‡] Masanori Kobayashi,[‡] Akihiko Sato,[‡] Matthew N. Johnson,[†] Edward P. Garvey,[†] and Tamio Fujiwara[‡]

[†]GlaxoSmithKline Research & Development, Infectious Diseases Therapeutic Area Unit, Five Moore Drive, Research Triangle Park, North Carolina 27709, United States

[‡]Shionogi Pharmaceutical Research Center, Shionogi & Co., Ltd., 3-1-1 Futaba-cho, Toyonaka-shi, Osaka 561-0825, Japan

Supporting Information

ABSTRACT: We report herein the discovery of the human immunodeficiency virus type-1 (HIV-1) integrase inhibitors dolutegravir (S/GSK1349572) (**3**) and S/GSK1265744 (**4**). These drugs stem from a series of carbamoyl pyridone analogues designed using a two-metal chelation model of the integrase catalytic active site. Structure−activity studies evolved a tricyclic series of carbamoyl pyridines that demonstrated properties indicative of once-daily dosing and superior potency against resistant viral strains. An inherent hemiaminal ring fusion stereocenter within the tricyclic carbamoyl pyridone scaffold led to a critical substrate controlled diastereoselective synthetic strategy whereby chiral information from small readily available amino alcohols was employed to control relative and absolute stereochemistry of the final drug candidates. Modest to extremely high levels of stereochemical control were observed depending on ring size and position of the stereocenter. This approach resulted in the discovery of **3** and **4**, which are currently in clinical development.

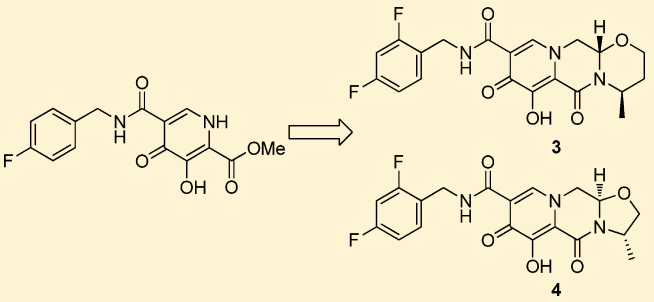

INTRODUCTION

HIV/AIDS remains a serious threat to public health worldwide. The latest UNAIDS report for the end of 2012 indicates the number of people living with HIV worldwide now resides at over 34 million.[1] This number has stabilized or grown slightly over the past few years, but unfortunately there are still approximately 2.5 million new infections annually and 1.7 million deaths. Antiretroviral (ARV) drugs have been one of the major advancements in medicine over the past 25 years and have turned HIV/AIDS into a manageable chronic disease. One notable recent development is the realization of HIV integrase inhibitors (INIs) as a new class of approved drugs. HIV-1 integrase (IN) is a virally encoded enzyme that catalyzes two biochemical reactions and is essential for replication. First, it catalyzes the removal of the terminal two nucleotides on the respective 3′ ends of the viral DNA (termed 3′ processing). Second, IN facilitates the nicking of host chromosomal DNA by the newly exposed 3′ hydroxyl moieties, resulting in strand transfer of the viral dsDNA. Integrase strand transfer inhibitors (INSTi's) have become an attractive drug target over the past few years, with numerous two-metal chelating scaffolds being pursued based on the pharmacophore shown in Figure 1.[2]

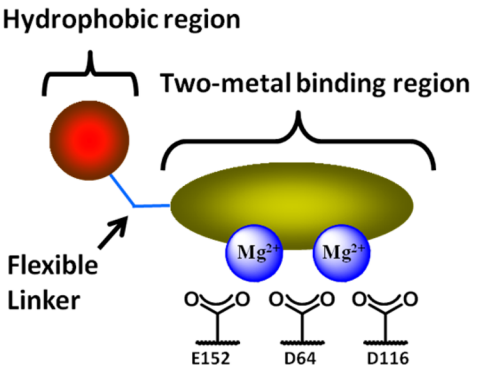

Figure 1. Two-metal binding pharmacophore model for HIV-1 integrase strand transfer inhibitors.

Two examples of metal-binding INSTi's are raltegravir (RAL, **1**) and elvitegravir (EVG, **2**), which received regulatory approval in 2007 and 2012, respectively (Figure 2). While these are both impressive new antiretrovirals and have established INSTi's as

Received: May 1, 2013
Published: June 25, 2013

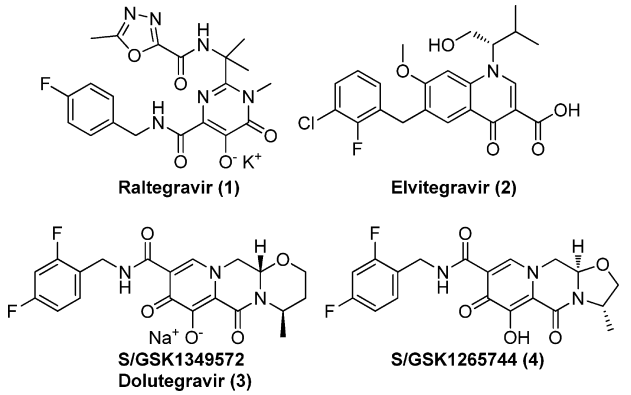

Figure 2. HIV-1 integrase strand transfer inhibitors.

valued components for combination antiretroviral therapy, they both have distinct limitations and leave room for meaningful improvements for patients. Raltegravir is the first-in-class INSTi but requires a high dose of 400 mg twice daily (BID).[3] In addition, three major IN signature mutation pathways result in substantial loss of potency of RAL (N155H, Y143C, and Q148H(R)(K)) and render it ineffective against these viruses.[4,5] EVG treatment engenders slightly different resistance pathways (T66I, E92Q, S147G, Q148H(R)(K), N155H), but there is extensive EVG cross resistance among RAL failures.[6] The major advance that EVG provides is the option for once daily dosing (QD). However, this requires the use of a pharmacokinetic (PK) boosting agent such as ritonavir or cobicistat to inhibit CYP3A4, which is a primary route of metabolism for EVG.[7] As a result of these limitations, our primary objective was to find a medicine that would allow once-daily doses (<100 mg) without the need for pharmacoenhancers (PK boosting), minimal drug−drug interaction potential, and importantly a lack of cross-resistance to existing agents.[8]

RESULTS AND DISCUSSION

We recently reported on the design and initial structure−activity relationship findings of a series of carbamoyl pyridone heterocycles.[9−11] This work progressed from initial monocyclic derivatives such as **5** into more elaborate bi- and tricyclic versions (e.g., **6**, **7**, and **8**) as shown in Figure 3. Monocyclic

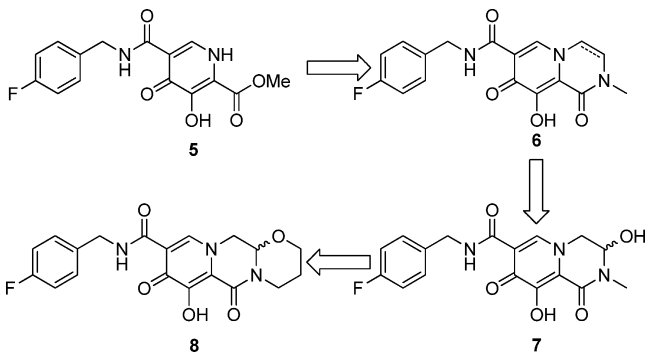

Figure 3. Evolution of the carbomoyl pyridone series.

analogue **5** served to validate the metal binding motif of the 3-hydroxy-4-oxo-2-carboxylic ester substituted pyridone system consistent with the pharmacophore model described in Figure 1. Positioning of the benzyl carboxamide at the pyridone 5 position provided the appropriate spatial relationship for the aromatic moiety required for potent inhibition of the integration strand transfer event. A key feature of this novel carbamoyl pyridone motif was the intentional use of a triad of all oxygen-derived lone pairs to serve as the chelating donor atoms toward the two divalent metals. This concept was derived from the hard/soft acid/base theory in order to match the harder oxygen atoms in the carbamoyl pyridone motif with the hard metal properties of the divalent magnesium cofactor. It was our hypothesis that previous scaffolds suffered from the less-than-optimal affinity of a borderline nitrogen lone pair for the hard Mg^{2+} cofactors, potentially leading to a less favorable and/or selective inhibition of the HIV-1 integrase catalytic activity. Cohen has recently shown a pyrone core to have superior inhibitory activity in an integrase biochemical assay when compared to several related scaffolds in a systematic study of a set of core heterocylic motifs.[12] The conclusions from his work about the importance of hard Lewis base donor character of the inhibitor are completely consistent with our hypotheses and findings from the current study and our previous work. The Cohen study has also suggested the relative orientation of one 5- and one 6- membered metalocyclic ring to the two magnesium ion positions was important. It is noteworthy that in the case of our system, the 5- and 6-membered rings formed upon metal coordination are reversed relative to the pyrone system studied due to the different positioning of the benzyl carboxamide.[13] While monocyclic analogues were potent, further enhancement of the structure was necessary to improve the resistance profile. Additionally, modification of the 2-ester substituent to the corresponding series of amides resulted in significant losses in activity, thus limiting the ability to optimize these small yet attractive structures. This ester to amide potency decrease was attributed to conformational barriers preventing the amide group from existing in a coplanar arrangement with the pyridone motif, thus preventing an optimal coordination of both Mg^{2+} simultaneously. The series evolved into bicyclic derivatives represented by structure **6**. The conformational challenges were relieved by this change and potency against wild-type (wt) virus restored, but key resistant mutations were still problematic. However, when the bicyclic system was further substituted with a hydroxyl moiety on the saturated piperazinone ring (e.g., **7**) significant improvements in the potency against a key integrase position 148 mutant (Q148K) were observed. Additionally, the addition of human serum (HS) to the antiviral assay to mimic the physiological environment resulted in only a modest decrease in activity. However, control of the new hydroxyl group's stereochemistry present in **7** during synthesis and its subsequent configurational integrity were problematic. We envisioned that a solution to the stability concerns of the hydroxyl group would be to tether it into a tricyclic system as in **8**.

CHEMISTRY AND SAR

The carbamoyl pyridone analogue **8**[10] containing a 6-membered hemiaminal ring was a potent antiviral in a pseudotyped virus assay ($^{pHIV}IC_{50}$ 1.9 nM).[14] Additionally, it had a modest serum protein-binding shift to give a protein-adjusted IC_{50} ($^{pHIV}PAIC_{50}$) of 20 nM in the pHIV assay system. In addition, data from a HeLa CD4 β-gal assay indicated only a 2.8-fold loss in activity against the Q148K mutant virus.[15] Although this virological profile was a significant advance toward our goal, the current data set was from the racemate. The individual isomers were isolated after chiral chromatographic separation of the *O*-benzyl protected precursor **10** (Scheme 1) to give the enantiopure benzyl ethers **10*R*** and **10*S***, and the absolute stereochemistry was assigned using

dx.doi.org/10.1021/jm400645w | J. Med. Chem. 2013, 56, 5901−5916

Scheme 1. Synthesis of Tricyclic Carbamoyl Pyridone 8[10,a]

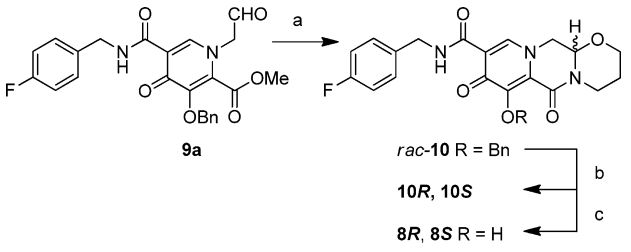

[a]Reagents and conditions: (a) 3-aminopropanol, AcOH, μW; (b) chiral SFC chromatography; (c) Pd/C, H_2, THF.

vibrational circular dichroism (VCD).[16] The benzyl ethers were subsequently deprotected through hydrogenolysis to give the individual enantiomers **8S** and **8R**.

Table 1 has comparison antiviral and low dose rat PK parameters for racemic **8** and its individual enantiomers **8S** and **8R**. We were initially concerned that the hemiaminal stability would be an issue, but no interconversion or chemical stability issues were observed with the purified isomers of **8**. Notably, the isomers had almost identical antiviral activity but significantly different protein binding shifts, with the *S* isomer showing a 43-fold shift while the *R* isomer had a very modest 4-fold loss of potency with added human serum albumin (HSA). The isomers also showed a differential loss of activity against the Q148K mutation, with the *S* derivative having only a 2.4-fold potency change while the *R* analogue had an 11-fold shift in activity. It is noteworthy that raltegravir (**1**) shows an 83-fold shift in this same assay system.[17,20] Both purified isomers as well as the parent racemate showed very low rat IV clearance values and good oral bioavailability, further stimulating our interest in the tricyclic series.

Although the data for the enantiomeric tricyclic analogues was encouraging, isolation of the individual stereoisomers through chiral chromatography was an unacceptable development hurdle. It was not apparent to us that there were sufficient synthetic chemistry approaches to reliably control the stereochemistry of a hemiaminal stereocenter especially in the context of the relatively complex ring system that we needed to build. The concept of a chiral auxiliary was among the first to be considered. However, adequate methodology or appropriate chemical handles to allow communication of the chiral information from an auxiliary to the requisite stereocenter was not evident. Consideration of the mechanism for the condensation and ring formation brought to mind the use of substrate control as a possible strategy to establish a handle to control stereochemistry as well as further evaluate structure–activity relationships (SAR). Our hope was that by adding chiral substitution to the system we would either improve or minimally maintain the biological activity or PK and also allow for robust stereocontrol of the hemiaminal. This concept is akin to an auxiliary approach whereby a diastereomeric environment is established to discriminate between isomers with the distinction that the auxiliary would be an integral part of the final drug. As shown in the top of Scheme 2, the use of an achiral amino alcohol in the synthesis of **10** results in no stereochemical preference in intermediate **A**, and thus racemic product is formed. However, as shown in the bottom of Scheme 2, if an amino alcohol with a pre-existing chiral center is employed, diastereomeric intermediates **B** and **C** have the potential to be formed, resulting in an equilibrium that should favor the most stable chair conformation as indicated by intermediate **C**. The final step of an effectively irreversible lactam ring closure should then lead to a biased product distribution related to the intermediates **B** and **C** in the most simple interpretation. Furthermore, the resulting products are formally diastereomers and separable by traditional achiral methods of crystallization or silica gel chromatography which would greatly improve purification. In the first attempt at this strategy using a racemic alcohol ***rac*-11**, a 9:1 diastereomeric ratio (dr) favoring the expected product **12** resulting from both the methyl and methylene hemiaminal substituents in equatorial orientations was observed. This initial experiment demonstrated the relative stereocontrol principle. We immediately repeated the reaction with highly enantiomerically pure alcohol **11** and obtained a matching optical purity of **12** after removal of the minor diastereomer by traditional chromatography. Thus, the stereocenter in the alcohol **11** formally dictated both the relative and absolute stereochemical outcome. Subsequent removal of the benzyl ether moiety via hydrogenolysis analogous to deprotection from Scheme 1 provided the active species **13** in diastereo and enantiomerically pure form. Because many small chiral nonracemic amino alcohols were available from the chiral pool with minimal modifications or can be accessed de novo through a variety of well established asymmetric synthetic methods, we

Table 1. Antiviral Activity and Pharmacokinetics for 8[10,a]

Compd	Structure	$^{pHIV}IC_{50}$ (nM) (95% CI)	$^{pHIV}PAIC_{50}$ (nM) (95% CI)	Q148K (FC)[b]	Cl (ml/min/kg)	F (%)
***rac*-8**	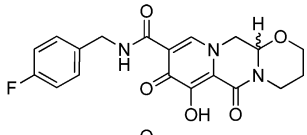	1.9 (0.5,7.1)	20 (13,31)	2.8	0.10	51
8*S*	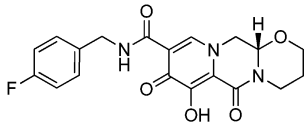	1.9 (0.4,9.6)	81 (12,540)	2.4	0.10	79
8*R*	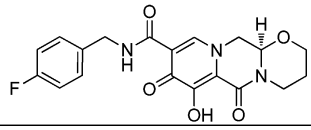	2.2 (1.4,3.5)	9.4 (3.6,25)	11	0.17	52

[a]Data represent the mean of at least three replicates. [b]Fold change against the resistant variant in a HeLa CD4 β-gal assay.

dx.doi.org/10.1021/jm400645w | J. Med. Chem. 2013, 56, 5901–5916

Scheme 2. Implementing Substrate Control of a Hemiaminal Stereocenter

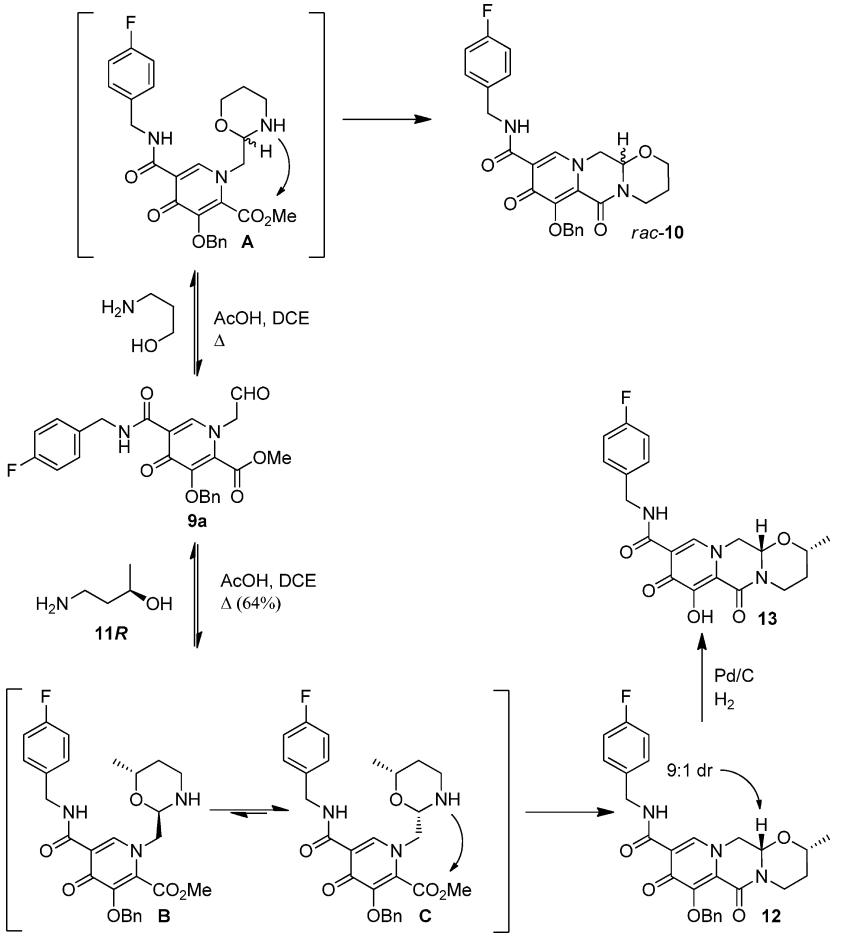

next examined the scope and limitations of this chemistry as well as developed the SAR of this tricyclic series.

The methyl isomer **13** was a potent inhibitor of the HIV-1 integrase function in both the biochemical strand transfer assay (5 nM) as well as a pHIV cell-based assay (2.1 nM) (Table 2). Interestingly, comparing to the analogous unsubstituted ring system in **8S**, methyl derivative **13** has an approximate 4-fold lower protein binding shift (12-fold for **13** vs 43 fold for **8S**). It is noted that an excellent window of activity versus cytotoxicity was observed throughout the series reported herein (data not shown). The enantiomeric compound **14** was also potent in the pHIV assay and showed a very low protein shift, consistent with the rank order of the *R* and *S* enantiomers of **8**. The corresponding 2,4-difluorobenzyl amides **15** and **16** had a similar profile but were slightly more potent overall. Extension of this from the methyl to ethyl and isopropyl gave similar synthetic chemistry results and largely indistinguishable antiviral activity within the expected assay variability. The trend of the *S* hemiaminal-containing isomer having a higher protein-adjusted antiviral activity held throughout the simple alkyl substituted analogues **17**–**20**. The series was briefly extended to more polar analogues **21** and **22**, which showed minimal activity losses with added HSA. In these examples, both enantiomers had an approximate 2-fold shift and were essentially indistinguishable in their biological activity. A 2-phenyl analogue (**23**) was examined and found to have a modest loss of activity compared to other members of the series in the absence of added protein and suffered substantially further in the presence of HSA. Data were collected on the difluoro benzyl set against the key Q148K mutant in the pseudo-HIV assay system as a preliminary SAR of the resistance profile. The methyl-containing analogues **15** and **16** displayed a minor 2–3-fold loss of potency as a result of the position 148 mutation. The trend was toward larger analogues with more lipophilic substitutions having a slightly increased fold-change against the Q148K mutation in the case of the *S* isomers while the *R* isomers remained more consistently in the 2–3-fold range. Overall, all of the analogues in the tricyclic series shown in Table 2 containing a 2-substituted 6-membered hemiaminal ring had a less than 9-fold loss in activity when challenged with the Q148K mutation, in contrast to the 77-fold change observed with raltegravir in the same assay system.[8,18]

We next moved to 3 substitution on the 6-membered hemiaminal ring. Condensing aldehyde **9b** with a 2-methyl propanolamine **24** provided the diequatorial product albeit in a modest 4:1 diastereoselectivity (eq 1). The biological activity of **28** and **29** was slightly improved over their 2-methyl counterparts (**13** and **14**). The protein shift was notably higher in **28** as potency increased to over 200 nM in the presence of added HSA (Table 3). Difluoro analogue **30** was essentially equipotent to the monofluoro compound **29**. The *gem*-dimethyl analogues **31** and **32** mentioned above were isolated via chiral separation of the racemic mixture in order to compare the impact of further substitution. As with the unsubstituted initial examples **10**, the benzyl ether precursors to **31** and **32** were used for absolute stereochemical assignment via vibrational circular dichroism (VCD).[16] These analogues again verified a large protein shift

dx.doi.org/10.1021/jm400645w | J. Med. Chem. 2013, 56, 5901–5916

Table 2. Effects of 2-Substitution on 6-Membered Ring Tricyclic Carbamoyl Pyridones[a]

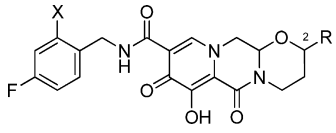

Compd	X	Structure	$^{pHIV}IC_{50}$ (nM) (95% CI)	$^{pHIV}PAIC_{50}$ (nM) (95% CI)	Q148K (FC)[b]
1	-	Ral	2.0 (1.4,2.9)	7.1 (3.0,9.9)	79
13	H	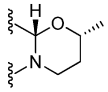	2.1 (2.0,2.3)	25 (20,30)	ND
14	H	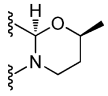	1.3[c]	3.3 (1.6,6.9)	ND
15	F	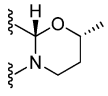	0.9 (0.7,1.1)	7.0 (2.1,23.2)	2.1
16	F	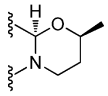	0.5 (0.4,0.7)	1.5 (0.8,2.7)	2.8
17	F	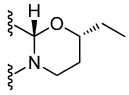	0.7 (0.7,0.8)	9.4 (6.6,13)	4.6
18	F	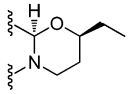	0.5 (0.4,0.6)	3.1 (1.7,5.4)	2.2
19	F	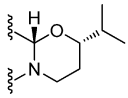	2.0 (1.1,3.7)	20 (17,22)	8.1
20	F	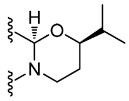	0.7 (0.6,0.8)	4.1 (2.8,6.2)	1.9
21	F	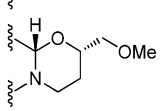	1.4 (1.2,1.5)	2.3 (1.0,5.3)	5.0
22	F	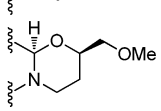	0.4 (0.3,0.5)	0.9 (0.5,1.6)	3.5
23	F	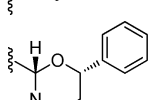	5.6 (3.4,10.0)	50 (27,94)	8.5

[a]Data represent the mean of three or more replicates. [b]Fold change against the resistant variant in the pHIV assay. [c]Data are from a single replicate.

from the *S* isomer **32**, similar to monomethyl analogue **28**, but were not attractive due to the loss of substrate control of chirality transfer as a result of the achiral starting amino-alcohol. The rank ordering of the *S* hemiaminal stereoisomers having a larger decrease in apparent potency in response to HSA was consistent through this series. The 3-methyl analogue **28** showed a larger 36-fold decrease in potency against Q148K virus compared to the 3-methyl derivative **29** (9.9-fold) decrease. The difluorobenzyl analogue **30** had a slight improvement in fold change in potency against the Q148K mutation compared to its

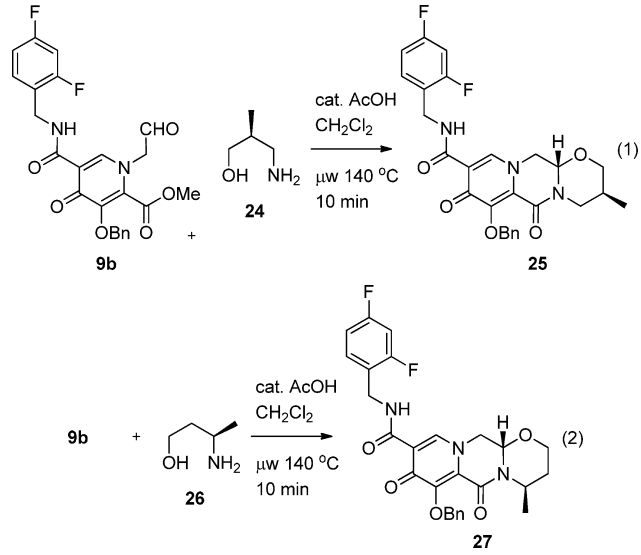

Table 3. Effects of 3- or 4-Substitution on 6-Membered Ring Tricyclic Carbamoyl Pyridones[a]

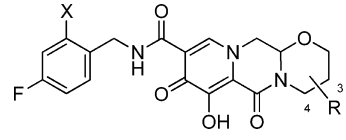

Compd	X	Structure	$^{pHIV}IC_{50}$ (nM) (95% CI)	$^{pHIV}PAIC_{50}$ (nM) (95% CI)	Q148K (FC)[b]
28	H	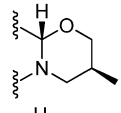	0.8 (0.4,1.6)	210 (120,350)	36
29	H	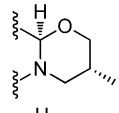	0.7 (0.5,0.9)	5.6 (4.5,6.9)	9.9
30	F	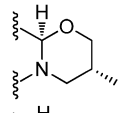	0.5 (0.4,0.5)	5.2 (2.8,9.7)	5.7
31	H	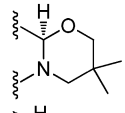	2.0 (1.1,3.3)	7.9 (3.7,16.7)	8.1
32	H	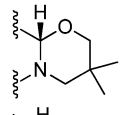	1.1 (0.9,1.5)	440 (290,670)	3.6
33	F	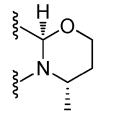	0.5 (0.5,0.6)	4.0 (2.1,7.7)	2.2
3	F	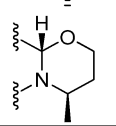	1.7 (1.3,2.2)	22 (15,33)	0.4

[a]Data represent the mean of at least three replicates. [b]Fold change against the resistant variant in the pHIV assay.

monofluoro counterpart **29**. In general, we observed the difluoro analogues to be as good or improved over the monofluoro and therefore more emphasis was placed on synthesis of the difluoro analogues. The *gem*-dimethyl enantiomers **31** and **32** had slightly

dx.doi.org/10.1021/jm400645w | J. Med. Chem. 2013, 56, 5901−5916

differing activities against the mutant but overall were not significant improvements over the more desirable diastereomeric members of the series.

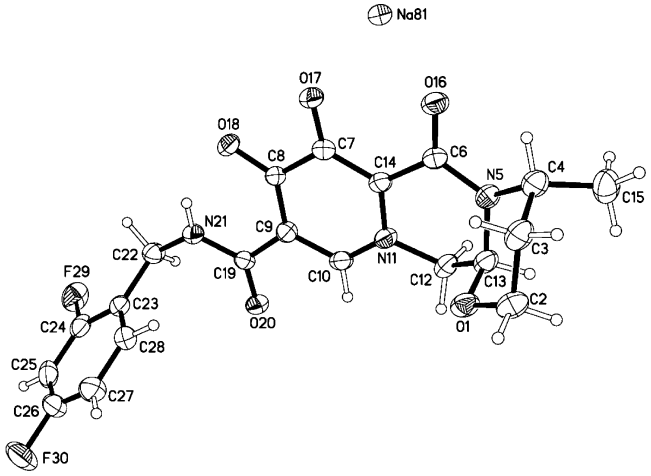

Figure 4. A view of one of the two anions and cations found in the asymmetric unit of the sodium salt of **3** from single crystal X-ray diffraction, showing the numbering scheme employed. Anisotropic atomic displacement ellipsoids for the non-hydrogen atoms are shown at the 50% probability level. Hydrogen atoms are displayed with an arbitrarily small radius. The absolute structure was unambiguously determined on the basis of anomalous dispersion effects, and this was shown to be the same for both independent anions (C4, *R*; C13, *S*). Coordinates have been deposited in the Cambridge Crystallographic Data Centre CCDC 935362.

We continued our exploration next at the 4-position. Condensation of **9b** with 3-methylpropanolamine **26** gave a 20:1 mixture favoring diastereomer **27** (eq 2). Removal of the benzyl group provided 4-methyl derivative **3**, the relative and absolute stereochemistry of which was confirmed by single crystal X-ray of the corresponding Na^+ salt. The relative stereochemistry consisted of a 1,3-diaxial relationship between the C4 methyl and C13 (hemiaminal) methine, with the newly formed C13 stereochemistry being assigned the *S* configuration as shown in Figure 4. This finding was at odds with the expected isomer containing an equatorial C4 methyl and *R* configuration of the C13 methine. However, upon closer analysis, the methyl group in the 4-position of the newly formed ring creates a significant steric interaction with the amide π system during the ring closure of the diequatorial major hemiaminal intermediate (Figure 5, TS2). As such, the Curtin–Hammett principle can be invoked to explain the equilibrating mixture of A and B proceeding through the lower transition state (TS1) to the observed product C. Interestingly, the 4-methyl group appears to provide sufficient steric bulk to drive high axial selectivity while remaining tolerant of the 1,3-diaxial interactions created by the C2 and C13 hydrogens to allow for good chemical conversion to the desired product **27** during the key condensation step.

As with the other regioisomeric 6-membered ring analogues, the 4-methyl derivatives **33** and **3** demonstrated potent antiviral activity in the pHIV assay system. The 4-methyl isomer **3** containing the *S* hemiaminal stereocenter again showed an elevated protein binding shift compared to the *R* counterpart **33**. In contrast, the potency against the Q148K mutant was slightly greater for enantiomer **3** versus **33**.

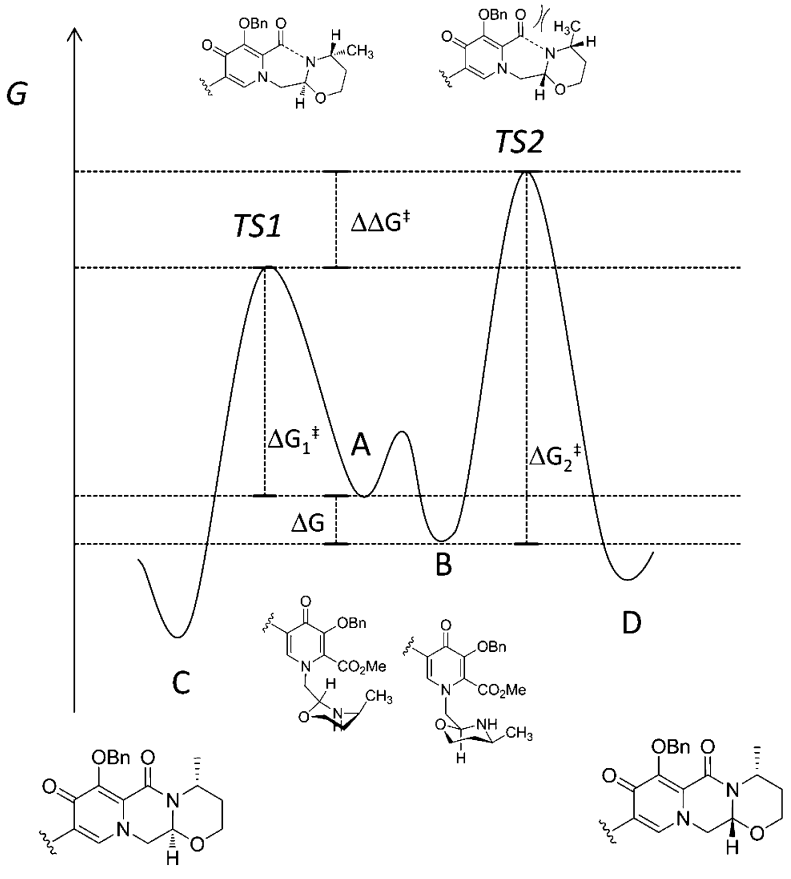

Figure 5. Curtin–Hammett explanation of 4-methyl substitution stereochemistry.

dx.doi.org/10.1021/jm400645w | *J. Med. Chem.* 2013, 56, 5901–5916

The survey of the ring condensation diastereoselectivity and subsequent SAR studies was extended to a series of 5-membered derivatives by reacting 1,2-amino-alcohols with aldehyde **9b**. The first attempt using 1-methyl-ethanolamine (**34**) resulted in a disappointing 3:1 mixture of diastereomers (eq 3). The isomers were not easily separable, and the mixture was not fully characterized to determine the stereochemical isomer ratio. However, when the regioisomeric 2-methyl-ethanolamine **36** was employed, a high level of diastereoselectivity was observed resulting in a diastereomeric ratio (dr) of greater than 40:1, favoring the antistereochemistry as depicted in intermediate **37** (eq 4). Hydrogenolysis as before yielded the desired final active inhibitors in excellent yield. We did not further pursue the 2-methyl analogues due to the poor diastereoselectivity and focused on the 3-substituted series. These were derived from reduction of α-amino acids, as well as a wide repertoire of de novo methodologies targeting both natural and non-natural amino acids and alcohols.

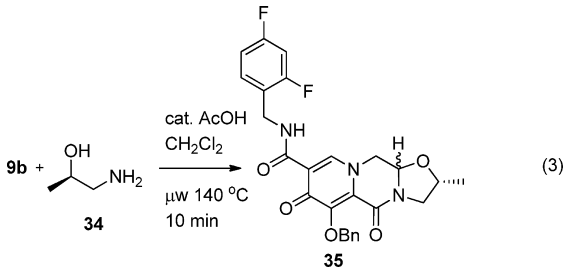

(3)

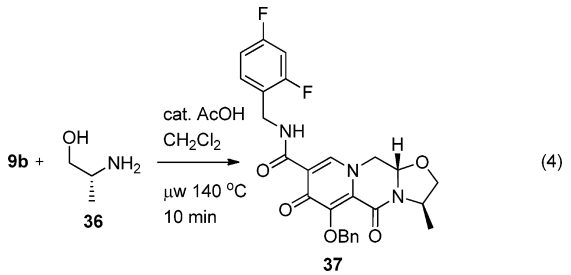

(4)

The condensation of 2-substituted ethanolamines to give 3-substituted 5-membered ring derivatives also resulted in high diastereoselectivities in all cases (Table 4). This included branched alkyl such as isopropyl and higher substitutions as found in compounds **42**–**46**. Heteroatom substitution was also well tolerated during the synthesis to provide alcohol and thioether analogues **50** and **51**, respectively. In the case of **50**, the condensation was performed with a benzyl protected *R*-serinol so as to avoid racemization from the *meso*-serinol hydroxyl groups in the unprotected form. Sulfone **52** was derived from the benzyl protected precursor thioether upon oxidation with *m*-CPBA and subsequent hydrogenolysis of the hydroxyl protecting group. Further evaluation of this chemistry employed phenylglycinol and phenylalaninol and resulted in the similar high diastereoselectivities as observed in the simple alkyl examples. These yielded the aryl containing derivatives **53**–**55**. The unprotected phenol and indole moieties from the L-tyrosine and L-tryptophan derived amino alcohols provided inhibitors **56** and **57**.

The 5-membered ring series delivered extremely potent antiviral activity from the unfunctionalized 3-alkyl derivatives. The 2-fluoro substituent improved the potency by approximately 4-fold in the case of the methyl analogues (**38** vs **4**) but performed less well in the *t*-butyl versions (**45** vs **46**). The products obtained from the small simple alkyl derived D-aminoalcohols (**39**, **41**, and **43**) appeared to have a lower fold shift in the presence of human serum albumin than the corresponding L derived products (**4**, **40**, and **42**). This would appear to be the opposite trend when compared to the 6-membered ring series. Branching of the alkyl group did not appear to have clear impact on the antiviral potency, perhaps as a result of competing potency and solubility properties. Alcohol **50** lost substantial potency (20-fold) compared to the methyl analogue **4**. Thioether **51** retained low nM potency with less loss of potency compared to **4**, however, it made up for this loss with an improved protein adjusted value. The sulfone **52** showed very poor activity with or without added proteins in the pHIV assay system. The rigid 3-phenyl derivative **53** was 143-fold less potent than the corresponding methyl analogue **4**, but the addition of a methylene bridge present in phenylmethyl derivative **55** appeared to restore or possibly improve potency over the corresponding methyl derivative **39**. It is also noteworthy that the protein shift of phenylmethyl analogue **55** and the methyl derivative **39** was just over 7-fold in each case. Neither the addition of the phenolic alcohol in **56** derived from tyrosine nor the indole group in **57** had an impact on activity and did not improve any properties to justify their increase in size and complexity over the methyl substitution in the original examples.

The Q148K mutant data for the 5-membered series consistently showed a sharp decline in potency against the mutant as the substituent present in the 5-membered saturated ring increased in size beyond a methyl group. Interestingly, tyrosine-derived phenol **56** was an exception, showing a very small potency change versus this mutant. The methyl derivative **4** performed best within the 5-membered ring series when potency, protein shift, and mutant profile were all taken into account. With exceptional sub-nM potency and just slightly higher fold change against the Q148K virus compared to the 6-membered ring series, **4** was deemed the most appropriate analogue for further progression. This minimal increase in Q148K fold change for **4** as compared to the 6-membered ring series was compensated for by the sub-nM activity against the wild-type virus, resulting in a $^{pHIV}IC_{50}$ of <2 nM against the Q148K variant in our screening assay system. Compound **4** did have a large protein shift (60-fold) in the presence of HSA, however, again this was attenuated by its intrinsic potency and the high protein binding may have a favorable impact on pharmacokinetic properties (for example, increasing half-life).

The ultimate pharmacokinetic goal of this program was once-daily dosing. Given that robust clinical antiviral efficacy depends on C_{trough} drug concentrations remaining above the protein-adjusted IC_{90}, we required that plasma concentrations of the test compounds remain above the protein-adjusted IC_{90} ($PAIC_{90}$) at the 24 h time point (C_{24h}) during early preclinical in vivo screening PK studies. For compound triaging, we used the experimentally determined factor of 4 to calculate the $PAIC_{90}$ from the existing pHIV $PAIC_{50}$. This efficacy target value was compared to the C_{24} from low oral dose (5 mg/kg) PK in rats. It was our goal to maximize this ratio of $C_{24h}/^{pHIV}PAIC_{90}$ as a means to take into account potency, protein shift, and in vivo PK profile as a measure to predict the best potential for robust efficacy. Many of the compounds from the above series achieved drug levels well in excess of the $^{pHIV}PAIC_{90}$ at 24 h post dose and would have been worthy of progression into higher species PK studies and additional evaluation. Two analogues of particular note were 6-membered ring derivative **3** and 5-membered ring analogue **4**, which gave 24 h coverage of the $^{pHIV}PAIC_{90}$ of 24-fold and 195-fold,[19] respectively, from 5 mg/kg oral doses of crystalline drug. These robust exposures also served to easily provide coverage for the protein-adjusted antiviral activities against the Q148K mutant. These screening PK data in conjunction with the compound's overall profile and somewhat different protein-binding properties

dx.doi.org/10.1021/jm400645w | J. Med. Chem. 2013, 56, 5901–5916

Table 4. Effects of 3-Substitution on 5-Membered Ring Tricyclic Carbamoyl Pyridones[a]

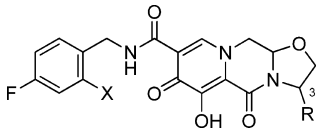

Compd	X	Structure	$^{pHIV}IC_{50}$ (nM) (95% CI)	$^{pHIV}PAIC_{50}$ (nM) (95% CI)	Q148K (FC)[b]
38	H	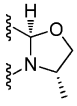	2.1 (1.5,2.8)	50 (38,65)	13
4	F	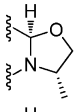	0.5 (0.4,0.7)	30 (21,45)	3.9
39	F	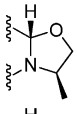	5.4 (1.8,16)	39 (18,86)	35
40	F	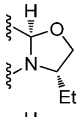	0.9 (0.7,1.1)	63 (48,83)	ND
41	F	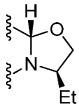	8.5 (2.0,11)	35 (12,110)	63
42	F	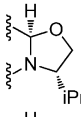	4.8 (2.3,9.8)	300 (110,790)	100
43	F	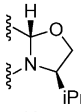	4.0 (2.4,6.7)	16 (7.9,33)	73
44	F	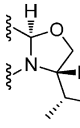	20 (9.6,41)	200 (81,480)	200
45	H	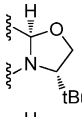	4.0 (3.3,4.8)	35 (23,52)	74
46	F	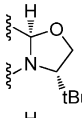	20 (4.0,97)	130 (31,540)	130
47	F	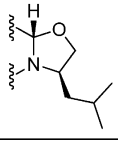	3.2 (2.2,4.6)	16 (8.5,29)	51
48	F	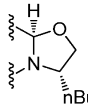	87 (11,660)	1800 (230,14000)	>57
49	F	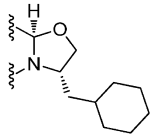	330 (57,2000)	3100 (540,18000)	>15
50	F	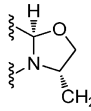	10 (6.4,16)	37 (9.7,140)	12
51	F	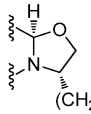	3.1 (2.6,38)	18 (9.6,33)	ND
52	F	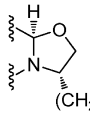	430 (270,680)	370 (170,790)	>10
53	F	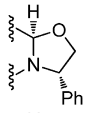	72 (45,110)	620 (120,3300)	44
54	F	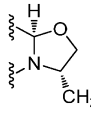	13 (3.0,62)	380 (37,3900)	13
55	F	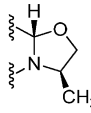	0.6 (0.4,1.0)	4.5 (3.3,6.4)	19
56	F	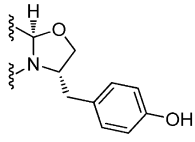	2.1 (1.4,3.2)	22 (14,35)	1.6
57	F	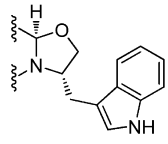	1.6 (1.1,2.2)	71 (51,99)	22

[a]Data represent the mean of at least three replicates. [b]Fold change against the resistant variant in the pHIV assay.

(reflected both in antiviral assay shift data and in equilibrium dialysis free fraction measurements (data not shown)) provided impetus to progress **3** and **4** for full virological and PK evaluation with the intention to progress both analogues into human trials if the data continued to support differentiation as outlined in our original goals.

VIROLOGY

Compounds **3** and **4** were examined in a biochemical integrase strand transfer assay (INST) as well as MT-4 cell and peripheral blood mononuclear cell (PBMC) HIV multiround replication assays (Table 5).[20,21] A more robust protein shift value was also determined via titrating in various concentrations of human

Table 5. Virological Profile of 3 and 4[a]

compd	INST (nM) (95% CI)	$^{MT4}IC_{50}$ (nM) (95% CI)	$^{PBMC}IC_{50}$ (nM) (95% CI)	100% HuS fold shift	$PAIC_{90}$ (ng/mL)
3	2.7 (1.7,4.1)	2.0 (0.8,5.1)	0.5 (0.3,0.8)	75	64
4	3.0 (2.1,4.4)	1.3 (0..6,2.5)	0.2 (0.1,0.4)	408	166

[a]Data represent the mean of at least three replicates.

dx.doi.org/10.1021/jm400645w | J. Med. Chem. 2013, 56, 5901−5916

serum into the MT-4 cell assay system and extrapolating the effect to 100% serum.[14] From these data, a better approximation of the protein adjusted clinical target was determined. The overall fold-shift values were somewhat higher than the pHIV data using purified HSA and suggested that these compounds may also bind serum proteins other than albumin. The two approaches were in qualitative agreement insofar as **4** showed a significantly higher fold-shift. Inhibition potency of viral replication in the multiround assays was in line with that determined in pHIV reporter system. The final clinical target was determined using the PBMC IC_{50} data and applying the 4-fold factor to approximate the IC_{90} and then applying the serum fold-shift factor. For **3** and **4**, the final $PAIC_{90}$ values were determined to be 64 and 166 ng/mL respectively.

Further evaluation of the resistance profile of **3** and **4** was undertaken in a HeLa cell assay using site-directed mutant viruses meant to profile the two lead structures against a panel of relevant raltegravir and elvitegravir signature mutations.[20,21] As can be seen in Figure 6, the fold change in activity when challenged with resistant mutations is vastly improved for **3** and **4** when compared with RAL and EVG. These results are consistent with the work of Cherepanov and Engelman wherein the prototype foamy virus surrogate of the HIV-1 integrase intasome was used for crystallographic studies to demonstrate how RAL, EVG, and **3** are likely to bind in the HIV-1 integrase active site.[22]

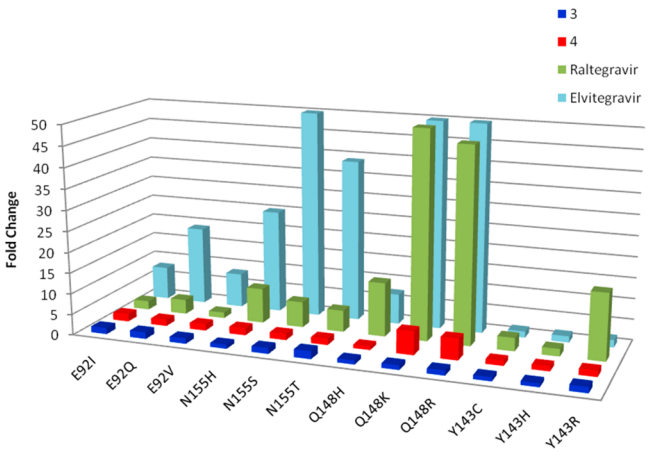

Figure 6. Comparison of Fold Change in HeLa cell IC_{50} of **3** and **4** Against Key IN Resistance Mutations.

IN VIVO AND IN VITRO PHARMACOKINETICS

The pharmacokinetic profiles of the two leads were determined for Sprague–Dawley rats, beagle dogs, and cynomolgus monkeys (Table 6). For the purpose of rigorous assessment, oral doses were performed using a standard 5 mg/kg dose from fully crystalline drug either as a suspension for **3** or in a capsule in the case of **4** to assess solid dosage form performance. For the purpose of this study, **3** was studied as its corresponding sodium salt while **4** was dosed as the neutral molecule. Values for the iv data for both compounds appear to correlate well with the free unbound fraction, resulting in higher clearance values (relative to the liver blood flow for a given species) from a larger unbound drug fraction. This is most pronounced in dogs for **3**, where a 4.6% free fraction results in clearance being approximately 7% of liver blood flow (lbf)[23] while for rats the clearance is extremely low (<0.5% lbf), corresponding to a much lower free drug fraction as determined by equilibrium dialysis measurements. The data for monkeys is in between the rat and dog at approximately 5% of lbf. Similar trends are present for **4**, although it has a lower free unbound fraction across all species with results in very low clearance. The data for rats are not reported due to extended exposures beyond 24 h, resulting in unreliable AUC values due to significant extrapolation. The oral bioavailability of **3** is good considering the "crystalline solid in a capsule" dose was not optimized. Despite lower oral bioavailability values measured for **4**, the C_{trough} target coverage of the $PAIC_{90}$ was still achieved across species. It is also noted that data presented for **4** are from a neutral formulation rather than a pH-adjusted formulation or more soluble salt of the acidic hydroxyl moiety. Both compounds were highly permeable (MDCK, P_{app} = 585 nm/s for **3**; 425 nm/s for **4**). However, solubility in simulated GI fluid was low (130 and 42 μg/mL for **3** and **4**, respectively), likely resulting in dissolution-limited absorption from our solid dose formulation studies. The chromatographic log $D_{7.4}$ values for **3** and **4** were measured to be 3.67 and 3.49, respectively.

No significant inhibition of CYP3A4 as well as no time dependent inhibition was observed for **3** or **4**. The compounds were also extremely stable ($T_{1/2}$ >180 min) in rat, dog, monkey, and human S9 fractions as well as rat and human hepatocyte incubations ($T_{1/2}$ >220 min). The combination of all the above PK data predicted that low QD oral doses (<100 mg/day) of both compounds in humans would achieve the targeted C_{trough} coverage of the $PAIC_{90}$.

Table 6. Pharmacokinetic Parameters for Rats, Dogs, and Cynomolgus Monkeys for 3 and 4[a]

compd	species	% unbound	Cl[e] (mL/min/kg)	$T_{1/2}$ (h)	Vdss (L/kg)	%F	$C_{24h}/PAIC_{90}$[c]
3	rat	0.1	0.23	6.2	0.1	34	18
3	dog[d]	4.6	2.2	5.2	0.3	35	4.6
3	cyno[d]	0.9	2.1	6.0	0.3	25	0.8
3	human	0.7					
4	rat	<0.1	NR[b]	>18	NR[b]	NR[b]	57
4	dog	0.7	0.34	5.7	0.14	8	0.9
4	cyno[d]	0.3	0.32	4.0	0.09	6.2	1.3
4	human	0.4					

[a]Data represent the mean of at least three replicates. [b]Not reportable due to prolonged exposure and extrapolation in excess of 20% of the total AUC. [c]The $PAIC_{90}$ value used was the clinical target of 64 ng/mL for **3** and 166 ng/mL for **4**. [d]Data represent the average of two independent experiments. [e]Liver blood flow (lbf) = 55/31/44 mL/min/kg for rat/dog/monkey[23]

dx.doi.org/10.1021/jm400645w | J. Med. Chem. 2013, 56, 5901–5916

CONCLUSION

The lead compounds **3** and **4** are known as S/GSK1349572 (S/GSK572, dolutegravir, DTG) and S/GSK1265744 (S/GSK744), respectively. Both compounds were progressed into rodent and nonrodent safety assessment studies and found to be suitable for clinical evaluation. The preclinical data presented herein have been validated as both **3** and **4** have shown robust low-dose once-daily PK and associated clinical efficacy. Compound **3** was selected to advance into phase III clinical evaluations using a 50 mg once daily dose for treatment naïve and experienced (but IN inhibitor naïve) HIV-infected patients and 50 mg twice daily for INI-resistant patients.[24] Additionally, compound **4** has achieved clinical proof of concept as an oral agent[25] and is being evaluated in long acting parenteral[26] formulations for once monthly or less frequent dosing to take advantage of its physicochemical and PK properties.

The use of diastereomeric control methodology to advance the initial tricyclic carbamoyl pyridone series into a chemically tractable lead optimization program has allowed for the discovery of two promising investigational drugs. By using clinically relevant viral mutations early in the compound triage, we have selected compounds that can add value in the clinical setting for both IN naïve and experienced patients wherein INI mutations may exist. Additionally, by choosing compounds with optimal potency and PK properties likely directly related to serum protein-binding effects, we have discovered INSTi's that have since been proven to be once-daily low-dose antiviral agents. Furthermore, in vitro metabolism and P450 data suggested early that both compounds would not be subject to significant P450-mediated metabolic pathways and would not require the codosing of a PK enhancer which is necessary for once-daily EVG. The lack of P450 inhibition by the carbamoyl pyridone scaffold is believed to predict a minimal risk for drug−drug interactions. In summary, we successfully developed multiple versions of tricyclic carbamoyl pyridone INSTi's to deliver two drugs that allow for unboosted low once-daily dosing as well as the novel paradigm of a long-acting approach for an HIV antiretroviral with **4**. Furthermore, these new INSTi's are potent against wild-type viruses and those containing RAL and EVG signature mutations, thus establishing further differentiation. Compounds **3** and **4** are poised to become valuable additions to the armamentarium of HIV antiretrovirals upon successful completion of their clinical evaluation.

EXPERIMENTAL SECTION

Compound Purity and Indentity. ^{1}H NMR spectra were recorded at 300 or 400 MHz. Melting points are uncorrected. Purities of test compounds were established by immediate processing quality control protocol (IPQC) to confirm identity and determine relative purity immediately before processing in the biological assays described (see Supporting Information for full details). IPQC analysis was by UPLC-MS with UV diode array detection to determine purity and MS used to confirm molecular weight. A Waters Acquity UPLC system comprising Binary Solvent manager, Sample Manager, PDA Detector, Waters ZQ or SQD mass spectrometer, Waters Acquity evaporative light scattering detector or Polymer Laboratories evaporative light scattering detector were employed. Mobile phases: acetonitrile + 0.1% formic acid, water + 0.1% formic acid. Wash solutions: strong wash 100% acetonitrile + 0.1% formic acid, weak wash 50:50 acetonitrile:-water + 0.1% formic acid. All individual lots of compounds tested were ≥95% pure (unless otherwise noted) according to these protocols (See Supporting Information, Table SI-2 for purity information). Analytical HPLC was also used in some cases to monitor reactions and establish final compound purity using a C-18 column (5.0 μm, 0→100% CH_3CN (or MeOH)/water with 0.05−0.1% HCOOH (or TFA)) and UV detection with or without mass spectrometer detection. Preparative HPLC conditions were as follows: C-18 column, 5 μm, 21.2 mm × 150 mm; flow rate = 4 mL/min; mobile phase: 10→100% CH_3CN/H_2O/0.1% HCOOH (10 min run). Combustion analysis was performed by Atlantic microlabs, Norcross, GA. Compounds **9a** and **9b** were prepared as previously described.[7]

(*R*)-7-(Benzyloxy)-*N*-(4-fluorobenzyl)-6,8-dioxo-3,4,6,8,12,12a-hexahydro-2*H*-pyrido[1′,2′:4,5]pyrazino[2,1-*b*][1,3]-oxazine-9-carboxamide (10*R*) and (*S*)-7-(Benzyloxy)-*N*-(4-fluorobenzyl)-6,8-dioxo-3,4,6,8,12,12a-hexahydro-2*H*-pyrido[1′,2′:4,5]-pyrazino[2,1-*b*][1,3]oxazine-9-carboxamide (10*S*). The enantiomers **10*R*** and **10*S*** were separated via preparative supercritical fluid chromatography (SFC) using a Novasep SuperSep 20−30 instrument with an OJ-H chiral column with 30% MeOH/CO_2 with a flow rate of 2 mL/min. Starting with 95 mg of *rac*-**10**,[10] provided 33 mg of the *R* isomer which eluted first and 28 mg of the *S* isomer. The absolute stereochemistry was assigned via vibrational circular dichroism (VCD) methods.[16] For **10*R***: ^{1}H NMR (400 MHz, $CDCl_3$) δ 10.41 (br s, 1 H), 8.36 (br s, 1 H), 7.62 (d, *J* = 7.0 Hz, 2 H), 7.44−7.22 (m, 5 H), 7.00 (t, *J* = 8.6 Hz, 2 H), 5.34−5.12 (m, 2 H), 4.92 (br s, 1 H), 4.77−4.48 (m, 3 H), 4.26 (d, *J* = 12.4 Hz, 1 H), 4.18−3.99 (m, 2 H), 3.76 (t, *J* = 11.1 Hz, 1 H), 3.01 (td, *J* = 2.7, 12.9 Hz, 1 H), 2.05−1.83 (m, 1 H), 1.59 (d, *J* = 13.7 Hz, 1 H).

(*S*)-*N*-(4-Fluorobenzyl)-7-hydroxy-6,8-dioxo-3,4,6,8,12,12a-hexahydro-2*H*-pyrido[1′,2′:4,5]pyrazino[2,1-*b*][1,3]oxazine-9-carboxamide (8*S*) and (*S*)-*N*-(4-Fluorobenzyl)-7-hydroxy-6,8-dioxo-3,4,6,8,12,12a-hexahydro-2*H*-pyrido[1′,2′:4,5]-pyrazino[2,1-*b*][1,3]oxazine-9-carboxamide (8*R*). A solution of **10*S*** (19.7 mg, 0.04 mmol) in THF (10 mL) was treated with 10% Pd/C (7 mg) and placed under 1 atm of H_2. Upon complete conversion, the mixture was filtered through Celite and triturated twice with Et_2O to provide **8*S*** (11 mg, 73%) as a white solid. ^{1}H NMR (400 MHz, chloroform-*d*) δ 12.37 (br s, 1 H), 10.39 (br s, 1 H), 8.35 (br s, 1 H), 7.37−7.18 (m, 2 H), 7.07−6.85 (m, 2 H), 5.05 (br s, 1 H), 4.83−4.47 (m, 3 H), 4.47−4.03 (m, 3 H), 3.98−3.73 (m, 1 H), 3.24−2.97 (m, 1 H), 2.16−1.90 (m, 1 H), 1.81−1.55 (m, 1 H). For **8R**: ^{1}H NMR (400 MHz, chloroform-*d*) δ 12.41 (br s, 1 H), 10.44 (br s, 1 H), 8.43 (br s, 1 H), 7.42−7.17 (m, 2 H), 7.09−6.87 (m, 2 H), 5.02 (br s, 1 H), 4.84−4.52 (m, 3 H), 4.44−4.10 (m, 3 H), 4.00−3.80 (m, 1 H), 3.25−3.00 (m, 1 H), 2.15−1.90 (m, 1 H), 1.82−1.59 (m, 1 H). LC/MS purity 96%. *m*/*z*, ES^+ LC/MS, *m*/*z* calcd 387.1, found 388.1 $(M + 1)^+$. For **8*S***: LC/MS purity 97%. LC/MS: *m*/*z* calcd 387.1, found 388.1 $(M + 1)^+$.

(2*R*,12a*S*)-7-(Benzyloxy)-*N*-(4-fluorobenzyl)-2-methyl-6,8-dioxo-3,4,6,8,12,12a-hexahydro-2*H*-[1,3]oxazino[3,2-*d*]pyrido-[1,2-*a*]pyrazine-9-carboxamide (12). To the solution of the compound **9a** (135 mg, 0.30 mmol) in dichloromethane (2 mL) (*S*)-4-aminobutan-2-ol (28 mg, 0.31 mmol) and acetic acid (10.0 mg, 0.17 mmol) were added. The reaction was performed with a microwave reaction apparatus at 140 °C for 10 min. After cooling to room temperature, the solvent was evaporated in vacuo and the residue was subjected to silica gel column chromatography, and fractions eluting with chloroform−methanol were collected and concentrated to obtain the product (138 mg, 94% yield) as colorless solid. ^{1}H NMR ($CDCl_3$) δ 10.46 (s, 1H), 8.40 (s, 1H), 7.62−7.66 (m, 2H), 7.31−7.41 (m, 5H), 7.00−7.07 (m, 2H), 5.30 (s, 2H), 5.01 (t, *J* = 3.9 Hz, 1H), 4.70−4.78 (m, 1H), 4.63 (d, *J* = 6.3 Hz, 2H), 4.30−4.36 (m, 1H), 4.11−4.12 (m, 1H), 3.82−3.94 (m, 1H), 3.05 (dt, *J* = 13.5, 4.2 Hz, 1H), 1.51−1.73 (m, 2H), 1.24 (d, *J* = 6.3 Hz, 1H).

(2*R*,12a*S*)-*N*-(4-Fluorobenzyl)-7-hydroxy-2-methyl-6,8-dioxo-3,4,6,8,12,12a-hexahydro-2*H*-pyrido[1′,2′:4,5]pyrazino[2,1-*b*][1,3]-oxazine-9-carboxamide (13) and (2*S*,12a*R*)-*N*-(4-Fluorobenzyl)-7-hydroxy-2-methyl-6,8-dioxo-3,4,6,8,12,12a-hexahydro-2*H*-pyrido[1′,2′:4,5]pyrazino[2,1-*b*][1,3]oxazine-9-carboxamide (14). ^{1}H NMR (DMSO-d_6) δ 12.48 (s, 1H), 10.36 (t, *J* = 6.0 Hz, 1H), 8.52 (s, 1H), 7.38−7.32 (m, 2H), 7.19−7.12 (m, 2H), 5.30 (t, *J* = 3.9 Hz, 1H), 4.52 (d, *J* = 6.0 Hz, 2H), 4.59−4.41 (m, 3H), 4.03−3.95 (m, 1H), 3.23 (td, *J* = 13.0, 2.8 Hz, 1H), 1.75 (d, *J* = 12.9 Hz, 1H), 1.50−1.35 (m, 1H), 1.15 (d, *J* = 6.0 Hz, 3H). ES^+ LC/MS: *m*/*z* calcd 401.14; for **13** found 402 $(M + 1)^+$, for **14** found 402 $(M + 1)^+$.

dx.doi.org/10.1021/jm400645w | J. Med. Chem. 2013, 56, 5901−5916

(2*R*,12a*S*)-*N*-(2,4-Difluorobenzyl)-7-hydroxy-2-methyl-6,8-dioxo-3,4,6,8,12,12a-hexahydro-2*H*-pyrido[1′,2′:4,5]pyrazino-[2,1-*b*][1,3]oxazine-9-carboxamide (15) and (2*S*,12a*R*)-*N*-(2,4-Difluorobenzyl)-7-hydroxy-2-methyl-6,8-dioxo-3,4,6,8,12,12a-hexahydro-2*H*-pyrido[1′,2′:4,5]pyrazino[2,1-*b*][1,3]oxazine-9-carboxamide (16). ^{1}H NMR (DMSO-d_6) δ 12.48 (s, 1H), 10.35 (t, J = 5.7 Hz, 1H), 8.50 (s, 1H), 7.44−7.35 (m, 1H), 7.29−7.20 (m, 1H), 7.10−7.03 (m, 1H), 5.30 (t, J = 3.9 Hz, 1H), 4.54 (d, J = 5.7 Hz, 2H), 4.58−4.42 (m, 3H), 4.06−3.95 (m, 1H), 3.29−3.18 (m, 1H), 1.75 (d, J = 13.8 Hz, 1H), 1.38 (m, 1H), 1.14 (d, J = 6.0 Hz, 3H). ES$^+$ LC/MS: m/z calcd 419.13; for **15** found 420.12 (M + 1)$^+$, for **16** found 420.10 (M + 1)$^+$.

(2*R*,12a*S*)-*N*-(2,4-Difluorobenzyl)-2-ethyl-7-hydroxy-6,8-dioxo-3,4,6,8,12,12a-hexahydro-2*H*-pyrido[1′,2′:4,5]pyrazino-[2,1-*b*][1,3]oxazine-9-carboxamide (17) and (2*S*,12a*R*)-*N*-(2,4-Difluorobenzyl)-2-ethyl-7-hydroxy-6,8-dioxo-3,4,6,8,12,12a-hexahydro-2*H*-pyrido[1′,2′:4,5]pyrazino[2,1-*b*][1,3]oxazine-9-carboxamide (18). ^{1}H NMR (DMSO-d_6) δ 12.48 (s, 1H), 10.34 (br s, 1H), 8.50 (s, 1H), 7.42−7.37 (m, 1H), 7.26−7.21 (m, 1H), 7.07−7.03 (m, 1H), 5.29 (s, 1H), 4.57−4.41 (m, 4H), 3.78−3.73 (m, 1H), 3.22 (t, J = 10.2 Hz, 1H), 1.75 (d, J = 10.8 Hz, 1H), 1.51−1.40 (m, 3H), 0.87 (d, J = 5.4 Hz, 3H). ES$^+$ LC/MS: m/z calcd 433.14; for **17** found 434.15 (M + 1)$^+$, for **18** found 434.12 (M + 1)$^+$.

(2*S*,12a*S*)-*N*-(2,4-Difluorobenzyl)-7-hydroxy-2-isopropyl-6,8-dioxo-3,4,6,8,12,12a-hexahydro-2*H*-pyrido[1′,2′:4,5]pyrazino-[2,1-*b*][1,3]oxazine-9-carboxamide (19) and (2*S*,12a*R*)-*N*-(2,4-Difluorobenzyl)-7-hydroxy-2-isopropyl-6,8-dioxo-3,4,6,8,12,12a-hexahydro-2*H*-pyrido[1′,2′:4,5]pyrazino[2,1-*b*]-[1,3]oxazine-9-carboxamide (20). ^{1}H NMR (DMSO-d_6) δ 12.48 (s, 1H), 10.35 (br s, 1H), 8.50 (s, 1H), 7.43−7.37 (m, 1H), 7.26−7.21 (m, 1H), 7.08−7.01 (m, 1H), 5.29 (s, 1H), 4.46−4.41 (m, 5H), 3.59−3.52 (m, 1H), 3.20 (t, J = 8.4 Hz, 1H), 1.78−1.72 (m, 1H), 1.69−1.57 (m, 1H), 1.49−1.41 (m, 1H), 0.86 (dd, J = 13.5, 4.8 Hz, 6H). ES$^+$ LC/MS: m/z calcd 447.16; for **19** found 448.14 (M + 1)$^+$, for **20** found 448.16 (M + 1)$^+$.

(2*S*,12a*S*)-*N*-(2,4-Difluorobenzyl)-7-hydroxy-2-(methoxymethyl)-6,8-dioxo-3,4,6,8,12,12a-hexahydro-2*H*-pyrido-[1′,2′:4,5]pyrazino[2,1-*b*][1,3]oxazine-9-carboxamide (21) and (2*R*,12a*R*)-*N*-(2,4-Difluorobenzyl)-7-hydroxy-2-(methoxymethyl)-6,8-dioxo-3,4,6,8,12,12a-hexahydro-2*H*-pyrido[1′,2′:4,5]-pyrazino[2,1-*b*][1,3]oxazine-9-carboxamide (22). ^{1}H NMR ($CDCl_3$) δ = 12.33 (br s, 1H), 10.38 (br s, 1H), 8.30 (s, 1H), 7.40−7.30 (m, 1H), 6.85−6.75 (m, 2H), 5.12 (s, 1H), 4.80−4.70 (m, 1H), 4.64 (d, J = 5.9 Hz, 1H), 4.36 (d, J = 10.1 Hz, 1H), 4.24 (d, J = 13.1 Hz, 1H), 4.11−4.00 (m, 1H), 3.50−3.35 (m, 2H), 3.37 (s, 3H), 3.21−3.09 (m, 1H), 1.80−1.60 (m, 2H). ES$^+$ LC/MS: m/z calcd 449.14; for **21** found 450.12 (M + 1)$^+$, for **22** found 450.14 (M + 1)$^+$.

(2*S*,12a*S*)-*N*-(2,4-Difluorobenzyl)-7-hydroxy-6,8-dioxo-2-phenyl-3,4,6,8,12,12a-hexahydro-2*H*-pyrido[1′,2′:4,5]-pyrazino[2,1-*b*][1,3]oxazine-9-carboxamide (23). ^{1}H NMR ($CDCl_3$) δ 12.45 (s, 1H), 10.38 (s, 1H), 8.50 (s, 1H), 7.42−7.21 (m, 7H), 7.08−7.04 (m, 1H), 5.51 (s, 1H), 4.98 (d, J = 8.7 Hz, 1H), 4.68−4.54 (m, 5H), 3.49 (t, J = 9.6 Hz, 1H), 1.98 (d, J = 9.6 Hz, 1H), 1.82−1.70 (m, 1H). ES$^+$ LC/MS: m/z calcd 481.14; found 482.17 (M + 1)$^+$.

(3*S*,12a*S*)-*N*-(4-Fluorobenzyl)-7-hydroxy-3-methyl-6,8-dioxo-3,4,6,8,12,12a-hexahydro-2*H*-pyrido[1′,2′:4,5]pyrazino-[2,1-*b*][1,3]oxazine-9-carboxamide (28) and (3*R*,12a*R*)-*N*-(4-Fluorobenzyl)-7-hydroxy-3-methyl-6,8-dioxo-3,4,6,8,12,12a-hexahydro-2*H*-pyrido[1′,2′:4,5]pyrazino[2,1-*b*][1,3]oxazine-9-carboxamide (29). ^{1}H NMR (DMSO-d_6) δ 12.45 (s, 1H), 10.36 (t, J = 5.9 Hz, 1H), 8.52 (s, 1H), 7.38−7.32 (m, 2H), 7.20−7.12 (m, 2H), 5.20 (t, J = 3.8 Hz, 1H), 4.52 (d, J = 5.9 Hz, 2H), 4.60−4.41 (m, 3H), 4.03−3.97 (m, 1H), 3.48 (t, J = 11.1 Hz, 1H), 2.86 (t, J = 12.5 Hz, 1H), 1.93−1.84 (m, 1H), 0.81 (d, J = 6.6 Hz, 3H). ES$^+$ LC/MS: m/z calcd 401.14; for **28** found 402.13 (M + 1)$^+$, for **29** found 402.14 (M + 1)$^+$.

(3*R*,12a*R*)-*N*-(2,4-Difluorobenzyl)-7-hydroxy-3-methyl-6,8-dioxo-3,4,6,8,12,12a-hexahydro-2*H*-pyrido[1′,2′:4,5]pyrazino-[2,1-*b*][1,3]oxazine-9-carboxamide (30). ^{1}H NMR ($CDCl_3$) δ 12.37 (s, 1H), 10.38 (br s, 1H), 8.31 (s, 1H), 7.40−7.32 (m, 1H), 6.84−6.80 (m, 2H), 4.98 (t, J = 3.7 Hz, 1H), 4.75−4.65 (m, 1H), 4.63 (d, J = 5.9 Hz, 2H), 4.38−4.30 (dd, J = 14.1, 4.0 Hz, 1H), 4.45−4.05 (m, 2H), 3.41 (dd, J = 12.9, 11.2 Hz, 1H), 2.70 (dd, J = 13.4, 11.6 Hz, 1H), 2.10−2.00 (m, 1H), 0.90 (d, J = 6.9 Hz, 3H). ES$^+$ LC/MS: m/z calcd 419.13; found 420.13 (M + 1)$^+$.

(*R*)-*N*-(4-Fluorobenzyl)-7-hydroxy-3,3-dimethyl-6,8-dioxo-3,4,6,8,12,12a-hexahydro-2*H*-[1,3]oxazino[3,2-*d*]pyrido[1,2-*a*]-pyrazine-9-carboxamide (31) and (*S*)-*N*-(4-Fluorobenzyl)-7-hydroxy-3,3-dimethyl-6,8-dioxo-3,4,6,8,12,12a-hexahydro-2*H*-[1,3]oxazino[3,2-*d*]pyrido[1,2-*a*]pyrazine-9-carboxamide (32). Methyl 3-(benzyloxy)-5-((4-fluorobengzyl)carbamoyl)-4-oxo-1-(2-oxoethyl)-1,4-dihydropyridine-2-carboxylate (**9a**) (29 mg, 0.064 mmol), 3-amino-2,2-dimethylpropan-1-ol (17 mg, 2.5 equiv), and 4 drops acetic acid were mixed in dichloroethane and heated at 80 °C for 1 h. The reaction was concentrated under reduced pressure, $NaHCO_3$ (aq) was added, and the mixture was extracted with dichloromethane, dried over sodium sulfate, and purified using silica-gel chromatography (0−100% EtOAc/hexanes, gradient elution). This material was separated using chiral SFC purification (40 mg) (50% methanol/carbon dioxide at 100 bar, 40 °C, 90 mL/min on an AD-H column) to give 12 mg of isomer 1 (first peak to elute) identified to be the *S* enantiomer and 12 mg peak 2 identified to be the *R* enantiomer. The peak 2 material, (*R*)-7-(benzyloxy)-*N*-(4-fluorobenzyl)-3,3-dimethyl-6,8-dioxo-3,4,6,8,12,12a-hexahydro-2*H*-pyrido[1′,2′:4,5]pyrazino[2,1-*b*][1,3]oxazine-9-carboxamide (7 mg), and 10 wt % Pd/C (13 mg) were dissolved in MeOH/THF, and the mixture was stirred at 1 atm H_2 for 20 min. The mixture was filtered through Celite and the pad was rinsed with dichloromethane/methanol until no product eluted, and the filtrate was concentrated under reduced pressure. The sample was suspended in methanol, and the solid was collected by vacuum filtrated to give desired product **31** (2 mg, 35%). ^{1}H NMR (400 MHz, $CDCl_3$) δ 12.39 (br s, 1H), 10.39 (m, 1H), 8.33 (s, 1H), 7.32 (m, 2H), 7.00 (t, J = 8.59 Hz, 2H), 4.97 (m, 1H), 4.66−4.55 (m, 2H), 4.44 (m, 1H), 4.34 (m, 1H), 4.18 (m, 1H), 3.71 (m, 1H), 3.57 (m,1H), 2.85 (d, J = 13.28 Hz, 1H), 1.14 − 0.92 (m, 6H). ES$^+$ LC/MS: m/z calcd 415.15; for **31** found 416.15 (M + 1)$^+$, for **32** found 416.14 (M + 1)$^+$.

(4*R*,12a*S*)-7-(Benzyloxy)-*N*-(2,4-difluorobenzyl)-4-methyl-6,8-dioxo-3,4,6,8,12,12a-hexahydro-2*H*-[1,3]oxazino[3,2-*d*]-pyrido[1,2-*a*]pyrazine-9-carboxamide (27). To the solution of the compound **9b** (705 mg, 1.50 mmol) in dichloromethane (10 mL), (*R*)-3-aminobutan-1-ol (200 mg, 2.24 mmol) and acetic acid (10.0 mg, 0.17 mmol) were added. The reaction was performed with a microwave reaction apparatus at 140 °C for 25 min. After cooling to room temperature, the solvent was evaporated in vacuo and the residue was subjected to silica gel column chromatography, and fractions eluting with chloroform−methanol were collected and concentrated to obtain the product (620 mg, 81% yield) as colorless solid. ^{1}H NMR ($CDCl_3$) δ 8:1.36 (d, J = 7.1 Hz, 4H), 1.50−1.55 (m, 1H), 2.16−2.18 (m, 1H), 3.98−3.99 (m, 2H), 4.11 (dd, J = 13.4, 6.0 Hz, 1H), 4.24 (dd, J = 13.5, 3.9 Hz, 1H), 4.66 (d, J = 5.9 Hz, 2H), 5.01−5.04 (m, 1H), 5.19 (dd, J = 6.0, 3.9 Hz, 1H), 5.29 (d, J = 10.2 Hz, 1H), 5.33(d, J = 9.9 Hz, 1H), 6.79−6.87 (m, 2H), 7.31−7.43 (m, 4H), 7.63−7.65 (m, 2H), 8.36 (s, 1H), 10.42 (s, 1H).

(4*R*,12a*S*)-*N*-(2,4-Difluorobenzyl)-7-hydroxy-4-methyl-6,8-dioxo-3,4,6,8,12,12a-hexahydro-2*H*-pyrido[1′,2′:4,5]pyrazino-[2,1-*b*][1,3]oxazine-9-carboxamide (3). To the solution of compound **A** (4.3 g, 8.40 mmol) in THF (120 mL), 10% palladium- carbon powder (400 mg) was added, and the mixture was stirred at room temperature for 1 h under hydrogen atmosphere. The reaction solution was filtered with Celite, and the filtrate was evaporated in vacuo. The residue was dissolved in chloroform, and insoluble residue was filtered with Celite again, and the filtrate was evaporated in vacuo. The residual crystals were recrystallized from dichloromethane−methanol to obtain the product (2.67 g, 76% yield). ^{1}H NMR ($CDCl_3$) δ 12.45 (s, 1H), 10.38 (br s, 1H), 8.30 (s, 1H), 7.40−7.30 (m, 1H), 6.85−6.75 (m, 2H), 5.26 (d, J = 5.8, 4.1 Hz, 2H), 5.05−4.95 (m, 1H), 4.64 (d, J = 5.9 Hz, 2H), 4.27 (dd, J = 13.4, 4.2 Hz, 1H), 4.12 (dd, J = 13.6, 6.0 Hz, 1H), 4.05 (t, J = 2.3 Hz, 1H), 4.02 (d, J = 2.2 Hz, 1H), 2.30−2.19 (m, 1H), 1.56 (dd, J = 14.0, 2.0 Hz, 1H), 1.42 (d, J = 7.0 Hz, 3H). ES$^+$ LC/MS: m/z calcd 419.13; found 420.13 (M + 1)$^+$.

(4*R*,12a*S*)-*N*-(2,4-Difluorobenzyl)-7-hydroxy-4-methyl-6,8-dioxo-3,4,6,8,12,12a-hexahydro-2*H*-pyrido[1′,2′:4,5]pyrazino-[2,1-*b*][1,3]oxazine-9-carboxamide (3) sodium salt. After dissolution of 18.0 g of compound **12** (1.0 equiv) in 54 mL of EtOH by heating, followed by filtration, 21.5 mL of 2N NaOHaq (1.0 equiv) was added to the solution at 80 °C. The solution was gradually cooled to

dx.doi.org/10.1021/jm400645w | J. Med. Chem. 2013, 56, 5901−5916

room temperature. Filtration, washing with 80 mL of EtOH, and drying provided 18.8 g of compound **13** (99% yield) as a crystal. ^{1}H NMR (DMSO-d_6) δ 10.70 (t, J = 6.0 Hz, 1H), 7.89 (s, 1 H), 7.40−7.30 (m, 1 H), 7.25−7.16 (m, 1H), 7.06−6.98 (m, 1H), 5.22−5.12 (m, 1H), 4.87−4.74 (m, 1H), 4.51 (d, J = 5.4 Hz, 2H), 4.35−4.25 (m, 1 H), 4.16 (dd, J = 1.8, 14.1 Hz, 1 H), 4.05−3.90 (m, 1H), 3.86−3.74 (m, 1 H), 2.00−1.72 (m, 1 H), 1.44−1.32 (m, 1 H), 1.24 (d, J = 6.9 Hz, 3H).

(4*S*,12a*R*)-*N*-(2,4-Difluorobenzyl)-7-hydroxy-4-methyl-6,8-dioxo-3,4,6,8,12,12a-hexahydro-2*H*-pyrido[1′,2′:4,5]pyrazino-[2,1-*b*][1,3]oxazine-9-carboxamide (33) and (4*R*,12a*S*)-*N*-(2,4-Difluorobenzyl)-7-hydroxy-4-methyl-6,8-dioxo-3,4,6,8,12,12a-hexahydro-2*H*-pyrido[1′,2′:4,5]pyrazino[2,1-*b*][1,3]oxazine-9-carboxamide (3). ^{1}H NMR ($CDCl_3$) δ 12.45 (s, 1H), 10.38 (br s, 1H), 8.30 (s, 1H), 7.40−7.30 (m, 1H), 6.85−6.75 (m, 2H), 5.26 (d, J = 5.8, 4.1 Hz, 2H), 5.05−4.95 (m, 1H), 4.64 (d, J = 5.9 Hz, 2H), 4.27 (dd, J = 13.4, 4.2 Hz, 1H), 4.12 (dd, J = 13.6, 6.0 Hz, 1H), 4.05 (t, J = 2.3 Hz, 1H), 4.02 (d, J = 2.2 Hz, 1H), 2.30−2.19 (m, 1H), 1.56 (dd, J = 14.0, 2.0 Hz, 1H), 1.42 (d, J = 7.0 Hz, 3H). ES$^+$ LC/MS: m/z calcd 419.13; found 420.11 (M + 1)$^+$.

(3*S*,11a*R*)-*N*-[(4-Fluorophenyl)methyl]-6-hydroxy-3-methyl-5,7-dioxo-2,3,5,7,11,11a-hexahydro[1,3]oxazolo[3,2-*a*]pyrido[1,2-*d*]-pyrazine-8-carboxamide (38). Compound **9a** (100 mg, 0.22 mmol) and (2*S*)-2-amino-1-propanol (0.10 mL, 1.28 mmol) were reacted in dichloromethane (2 mL) with acetic acid to give (3*S*,11a*R*)-*N*-[(4-fluorophenyl)methyl]-3-methyl-5,7-dioxo-6-[(phenylmethyl)oxy]-2,3,5,7,11,11a-hexahydro[1,3]oxazolo[3,2-*a*]pyrido[1,2-*d*]pyrazine-8-carboxamide (100 mg, 95%). This material was hydrogenated in a second step to give **38** (80 mg, 99%) as a white solid. ^{1}H NMR ($CDCl_3$) δ 11.43 (br, 1H), 10.28 (br, 1H), 8.35 (s, 1H), 7.28 (m, 2H), 6.97 (m, 2H), 5.29 (m, 1H), 4.55−4.38 (m, 5H), 3.89 (apparent t, J = 10.8 Hz, 1H), 3.70 (m, 1H), 1.45 (d, J = 5.6 Hz, 3 H). ES$^+$ LC/MS: m/z calcd 387.12; found 388.11 (M + 1)$^+$.

(3*S*,11a*R*)-*N*-[(2,4-Difluorophenyl)methyl]-6-hydroxy-3-methyl-5,7-dioxo-2,3,5,7,11,11a-hexahydro[1,3]oxazolo[3,2-*a*]pyrido[1,2-*d*]pyrazine-8-carboxamide Sodium Salt (4). Compound **9b** (510 mg, 1.08 mmol) and (2*S*)-2-amino-1-propanol (0.17 mL, 2.17 mmol) were reacted in 1,2-dichloroethane (20 mL) with acetic acid to give (3*S*,11a*R*)-*N*-[(2,4-difluorophenyl)methyl]-3-methyl-5,7-dioxo-6-[(phenylmethyl)oxy]-2,3,5,7,11,11a-hexahydro[1,3]oxazolo[3,2-*a*]-pyrido[1,2-*d*]pyrazine-8-carboxamide (500 mg, 93%). This material was hydrogenated in a second step to give **4** (386 mg, 94%) as a tinted white solid. ^{1}H NMR ($CDCl_3$) δ 11.46 (m, 1H), 10.28 (m, 1H), 8.32 (s, 1H), 7.35 (m, 1H), 6.80 (m, 2H), 5.30 (dd, J = 10.0, 4.0 Hz, 1H), 4.63 (m, 2H), 4.48−4.37 (m, 3H), 3.91 (dd, J = 12.0, 10.0 Hz, 1H), 3.73 (m, 1H), 1.48 (d, J = 6.0 Hz, 3H). ES$^+$ MS: 406 (M + 1).

(3*S*,11a*R*)-*N*-[(2,4-Difluorophenyl)methyl]-6-hydroxy-3-methyl-5,7-dioxo-2,3,5,7,11,11a-hexahydro[1,3]oxazolo[3,2-*a*]pyrido[1,2-*d*]pyrazine-8-carboxamide (4) Sodium Salt. (3*S*,11a*R*)-*N*-[(2,4-Difluorophenyl)methyl]-6-hydroxy-3-methyl-5,7-dioxo-2,3,5,7,11,11a-hexahydro[1,3]oxazolo[3,2-*a*]pyrido[1,2-*d*]-pyrazine-8-carboxamide (385 mg, 0.95 mmol) was treated with sodium hydroxide (0.95 mL, 1.0 M, 0.95 mmol) in ethanol (15 mL) so as to provide its corresponding sodium salt (381 mg, 94%) as a white solid. ^{1}H NMR (DMSO-d_6) δ 10.66 (m, 1H), 7.93 (s, 1H), 7.33 (m, 1H), 7.20 (m, 1H), 7.01 (m, 1H), 5.19 (m, 1H), 4.59 (m, 1H), 4.48 (m, 2H), 4.22 (m, 2H), 3.75 (m, 1H), 3.57 (m, 1H), 1.24 (d, J = 5.6 Hz, 3H). ES$^+$ LC/MS: m/z calcd 405.11; found 406.10 (M + 1)$^+$.

(3*R*,11a*S*)-*N*-[(2,4-Difluorophenyl)methyl]-6-hydroxy-3-methyl-5,7-dioxo-2,3,5,7,11,11a-hexahydro[1,3]oxazolo[3,2-*a*]pyrido[1,2-*d*]pyrazine-8-carboxamide Sodium Salt (39). To a solution of **9b** (409 mg, 0.87 mmol) in dichloroethane (20 mL) was added (2*R*)-2-amino-1-propanol (0.14 mL, 1.74 mmol) and 10 drops of glacial acetic acid. The resultant solution was heated at reflux for 2 h. Upon cooling, Celite was added to the mixture and the solvents removed in vacuo, and the material was purified via silica gel chromatography (2% CH_3OH/CH_2Cl_2 gradient elution) to give (3*R*,11a*S*)-*N*-[(2,4-difluorophenyl)methyl]-3-methyl-5,7-dioxo-6-[(phenylmethyl)oxy]-2,3,5,7,11,11a-hexahydro[1,3]oxazolo[3,2-*a*]pyrido[1,2-*d*]pyrazine-8-carboxamide (396 mg, 92%) as a glass. ^{1}H NMR ($CDCl_3$) δ 10.38 (m, 1H), 8.42 (s, 1H), 7.54−7.53 (m, 2H), 7.37−7.24 (m, 4H), 6.83−6.76 (m, 2H), 5.40 (d, J = 10.0 Hz, 1H), 5.22 (d, J = 10.0 Hz, 1H), 5.16 (dd, J = 9.6, 6.0 Hz, 1H), 4.62 (m, 2H), 4.41 (m, 1H), 4.33−4.30 (m, 2H), 3.84 (dd, J = 12.0, 10.0 Hz, 1H), 3.63 (dd, J = 8.4, 7.2 Hz, 1H), 1.37 (d, J = 6.0 Hz, 3H). ES$^+$ MS: 496 (M + 1). To a solution of this material (396 mg, 0.80 mmol) in methanol (30 mL) was added 10% Pd/C (25 mg). Hydrogen was bubbled through the reaction mixture via a balloon for 2 h. The resultant mixture was filtered through Celite with methanol and dichloromethane. The filtrate was concentrated in vacuo to give **39** as a pink-tinted white solid (278 mg, 86%). ^{1}H NMR ($CDCl_3$) δ 11.47 (m, 1H), 10.29 (m, 1H), 8.32 (s, 1H), 7.36 (m, 1H), 6.82 (m, 2H), 5.31 (dd, J = 9.6, 3.6 Hz, 1H), 4.65 (m, 2H), 4.47−4.38 (m, 3H), 3.93 (dd, J = 12.0, 10.0 Hz, 1H), 3.75 (m, 1H), 1.49 (d, J = 5.6 Hz, 3H). ES$^+$ MS: 406 (M + 1). The above material (278 mg, 0.66 mmol) was taken up in ethanol (10 mL) and treated with 1N sodium hydroxide (aq) (0.66 mL, 0.66 mmol). The resulting suspension was stirred at room temperature for 30 min. Ether was added, and the liquids were collected to provide the sodium salt of the title compound as a white powder (291 mg, 99%). ^{1}H NMR (DMSO-d_6) δ 10.68 (m, 1H), 7.90 (s, 1H), 7.35 (m, 1H), 7.20 (m, 1H), 7.01 (m, 1H), 5.20 (m, 1H), 4.58 (m, 1H), 4.49 (m, 2H), 4.22 (m, 2H), 3.74 (dd, J = 11.2, 10.4 Hz, 1H), 3.58 (m, 1H), 1.25 (d, J = 4.4 Hz, 3H). ES$^+$ LC/MS: m/z calcd 405.11; found 406.19 (M + 1)$^+$.

(3*S*,11a*R*)-*N*-[(2,4-Difluorophenyl)methyl]-3-ethyl-6-hydroxy-5,7-dioxo-2,3,5,7,11,11a-hexahydro[1,3]oxazolo[3,2-*a*]-pyrido[1,2-*d*]pyrazine-8-carboxamide (40). Compound **9b** (40 mg, 0.09 mmol) and (2*S*)-2-amino-1-butanol (0.1 mL) were reacted in dichloromethane (2 mL) with acetic acid to give (3*S*,11a*R*)-*N*-[(2,4-difluorophenyl)methyl]-3-ethyl-5,7-dioxo-6-[(phenylmethyl)oxy]-2,3,5,7,11,11a-hexahydro[1,3]oxazolo[3,2-*a*]pyrido[1,2-*d*]pyrazine-8-carboxamide (39 mg, 90%). This material was hydrogenated in a second step to give **40** (37 mg, 99%) as a tinted white solid. ^{1}H NMR ($CDCl_3$) δ = 11.47 (br, 1H), 10.26 (m, 1H), 8.35 (s, 1H), 7.32 (m, 1H), 6.77 (m, 2H), 5.29 (m, 1H), 4.60 (m, 2H), 4.47−4.32 (m, 3H), 3.93−3.85 (m, 2H), 2.08 (m, 1H), 1.68 (m, 1H), 0.95 (t, J = 7.6 Hz, 3H). ES$^+$ LC/MS: m/z calcd 419.13; found 420.29 (M + 1)$^+$.

(3*R*,11a*S*)-*N*-[(2,4-Difluorophenyl)methyl]-3-ethyl-6-hydroxy-5,7-dioxo-2,3,5,7,11,11a-hexahydro[1,3]oxazolo[3,2-*a*]-pyrido[1,2-*d*]pyrazine-8-carboxamide (41). Compound **9b** (40 mg, 0.09 mmol) and (2*R*)-2-amino-1-butanol (0.02 mL, 0.21 mmol) were reacted in dichloromethane (2 mL) with acetic acid to give (3*R*,11a*S*)-*N*-[(2,4-difluorophenyl)methyl]-3-ethyl-5,7-dioxo-6-[(phenylmethyl)-oxy]-2,3,5,7,11,11a-hexahydro[1,3]oxazolo[3,2-*a*]pyrido[1,2-*d*]-pyrazine-8-carboxamide (40 mg, 93%). This material was hydrogenated in a second step to give **41** (30 mg, 91%) as a white solid. ^{1}H NMR ($CDCl_3$) δ = 11.49 (br, 1H), 10.28 (m, 1H), 8.35 (s, 1H), 7.34 (m, 1H), 6.79 (m, 2H), 5.30 (m, 1H), 4.62 (m, 2H), 4.45−4.32 (m, 3H), 3.93−3.86 (m, 2H), 2.11 (m, 1H), 1.65 (m, 1H), 0.98 (t, J = 7.6 Hz, 3H). ES$^+$ LC/MS: m/z calcd 419.13; found 420.03 (M + 1)$^+$.

(3*S*,11a*R*)-*N*-[(2,4-Difluorophenyl)methyl]-6-hydroxy-3-(1-methylethyl)-5,7-dioxo-2,3,5,7,11,11a-hexahydro[1,3]oxazolo-[3,2-*a*]pyrido[1,2-*d*]pyrazine-8-carboxamide. (42). Compound **9b** (42 mg, 0.09 mmol) and (2*S*)-2-amino-3-methyl-1-butanol (0.1 mL) were reacted in 1,2-dichloroethane (8 mL) with acetic acid to give (3*S*,11a*R*)-*N*-[(2,4-difluorophenyl)methyl]-3-(1-methylethyl)-5,7-dioxo-6-[(phenylmethyl)oxy]-2,3,5,7,11,11a-hexahydro[1,3]oxazolo-[3,2-*a*]pyrido[1,2-*d*]pyrazine-8-carboxamide (40 mg, 86%). This material was hydrogenated in a second step to give **42** (34 mg, 99%) as a white solid. ^{1}H NMR ($CDCl_3$) δ = 10.29 (br, 1H), 8.36 (s, 1H), 7.33 (m, 1H), 6.79 (m, 2H), 5.29 (d, J = 6.4 Hz, 1H), 4.61 (m, 2H), 4.44 (d, J = 9.6 Hz, 1H), 4.34 (m, 1H), 4.17 (m, 1H), 4.02 (dd, J = 8.4, 5.2 Hz, 1H), 3.86 (m, 1H), 2.37 (m, 1H), 0.97 (m, 6H). ES$^+$ LC/MS: m/z calcd 433.14; found 434.14 (M + 1)$^+$.

(3*R*,11a*S*)-*N*-[(2,4-Difluorophenyl)methyl]-6-hydroxy-3-(1-methylethyl)-5,7-dioxo-2,3,5,7,11,11a-hexahydro[1,3]oxazolo-[3,2-*a*]pyrido[1,2-*d*]pyrazine-8-carboxamide (43). Compound **9b** (40 mg, 0.09 mmol) and (2*R*)-2-amino-3-methyl-1-butanol (0.1 mL) were reacted in 1,2-dichloroethane (8 mL) with acetic acid to give (3*R*,11a*S*)-*N*-[(2,4-difluorophenyl)methyl]-3-(1-methylethyl)-5,7-dioxo-6-[(phenylmethyl)oxy]-2,3,5,7,11,11a-hexahydro[1,3]oxazolo-[3,2-*a*]pyrido[1,2-*d*]pyrazine-8-carboxamide (41 mg, 92%). This material was hydrogenated in a second to give **43** (32 mg, 94%) as a white solid. ^{1}H NMR ($CDCl_3$) δ = 11.42 (br, 1H), 10.27 (br, 1H), 8.34 (s, 1H), 7.31 (m, 1H), 6.78 (m, 2H), 5.28 (d, J = 6.0 Hz, 1H), 4.60 (m, 2H),

4.42 (m, 1H), 4.33 (m, 1H), 4.16 (m, 1H), 4.01 (dd, J = 8.8, 5.2 Hz, 1H), 3.85 (m, 1H), 2.37 (m, 1H), 0.97 (d, J = 6.8 Hz, 3H), 0.95 (d, J = 6.4 Hz, 3H). ES$^+$ LC/MS: m/z calcd 433.14; found 434.14 (M + 1)$^+$.

(3*S*,11a*R*)-*N*-[(2,4-Difluorophenyl)methyl]-6-hydroxy-3-[(1*S*)-1-methylpropyl]-5,7-dioxo-2,3,5,7,11,11a-hexahydro[1,3]-oxazolo[3,2-*a*]pyrido[1,2-*d*]pyrazine-8-carboxamide Sodium Salt (44). 9b (417 mg, 0.89 mmol) and L-isoleucinol (259 mg, 2.21 mmol) were reacted in 1,2-dichloroethane (40 mL) with acetic acid to give (3*S*,11a*R*)-*N*-[(2,4-difluorophenyl)methyl]-3-[(1*S*)-1-methylpropyl]-5,7-dioxo-6-[(phenylmethyl)oxy]-2,3,5,7,11,11a-hexahydro-[1,3]oxazolo[3,2-*a*]pyrido[1,2-*d*]pyrazine-8-carboxamide (426 mg, 90%). This material was hydrogenated in a second step to give the corresponding sodium salt of **44** (384 mg, 99%) as a white solid. ^{1}H NMR (DMSO-d_6) δ 10.82 (m, 1H), 7.80 (m, 1H), 7.33 (m, 1H), 7.18 (m, 1H), 7.00 (m, 1H), 5.14 (m, 1H), 4.47 (d, J = 5.6 Hz, 2H), 4.31 (m, 1H), 4.18 (m, 1H), 3.96 (m, 1H), 3.84 (m, 1H), 3.71 (m, 1H), 3.40 (m, 1H), 1.88 (m, 1H), 1.36 (m, 1H), 1.04 (m, 1H), 0.85 (t, J = 7.2 Hz, 3H), 0.80 (d, J = 6.8 Hz, 3H). ES$^+$ LC/MS: m/z calcd 447.16; found 448.06 (M + 1)$^+$.

(3*S*,11a*R*)-3-(1,1-Dimethylethyl)-*N*-[(4-fluorophenyl)methyl]-6-hydroxy-5,7-dioxo-2,3,5,7,11,11a-hexahydro[1,3]oxazolo-[3,2-*a*]pyrido[1,2-*d*]pyrazine-8-carboxamide (45). 9a (41 mg, 0.09 mmol) and freebased L-*tert*-leucinol (59 mg, 0.50 mmol) were reacted in dichloromethane (2 mL) with acetic acid to give (3*S*,11a*R*)-3-(1,1-dimethylethyl)-*N*-[(4-fluorophenyl)methyl]-5,7-dioxo-6-[(phenylmethyl)oxy]-2,3,5,7,11,11a-hexahydro[1,3]oxazolo[3,2-*a*]-pyrido[1,2-*d*]pyrazine-8-carboxamide (40 mg, 85%). This material was hydrogenated in a second step to give **45** (32 mg, 97%) as a tinted white solid. ^{1}H NMR ($CDCl_3$) δ 11.15 (br, 1H), 10.32 (s, 1H), 8.38 (s, 1H), 7.29 (m, 2H), 6.98 (m, 2H), 5.43 (m, 1H), 4.58 (m, 2H), 4.36 (m, 2H), 4.21 (m, 1H), 3.99 (, 1H), 3.79 (m, 1H), 1.02 (s, 9H). ES$^+$ LC/MS: m/z calcd 429.17; found 430.14 (M + 1)$^+$.

(3*S*,11a*R*)-*N*-[(2,4-Difluorophenyl)methyl]-3-(1,1-dimethylethyl)-6-hydroxy-5,7-dioxo-2,3,5,7,11,11a-hexahydro[1,3]-oxazolo[3,2-*a*]pyrido[1,2-*d*]pyrazine-8-carboxamide (46). 9b (41 mg, 0.09 mmol) and freebased L-*tert*-leucinol (59 mg, 0.50 mmol) were reacted in dichloromethane (2 mL) with acetic acid to give (3*S*,11a*R*)-*N*-[(2,4-difluorophenyl)methyl]-3-(1,1-dimethylethyl)-5,7-dioxo-6-[(phenylmethyl)oxy]-2,3,5,7,11,11a-hexahydro[1,3]oxazolo-[3,2-*a*]pyrido[1,2-*d*]pyrazine-8-carboxamide (40 mg, 86%). This material was hydrogenated in a second step to give **46** (33 mg, 99%) as a tinted white solid. ^{1}H NMR ($CDCl_3$) δ 10.29 (s, 1H), 8.37 (s, 1H), 7.34 (m, 1H), 6.79 (m, 2H), 5.43 (m, 1H), 4.62 (m, 2H), 4.36 (m, 2H), 4.21 (m, 1H), 3.99 (, 1H), 3.81 (m, 1H), 1.03 (s, 9H). ES$^+$ LC/MS: m/z calcd 447.16; found 448.29 (M + 1)$^+$.

(3*R*,11a*S*)-*N*-[(2,4-Difluorophenyl)methyl]-6-hydroxy-3-(2-methylpropyl)-5,7-dioxo-2,3,5,7,11,11a-hexahydro[1,3]-oxazolo[3,2-*a*]pyrido[1,2-*d*]pyrazine-8-carboxamide (47). 9b (32 mg, 0.07 mmol) and (2*R*)-2-amino-4-methyl-1-pentanol (0.1 mL) were reacted in dichloromethane (2 mL) with acetic acid to give (3*R*,11a*S*)-*N*-[(2,4-difluorophenyl)methyl]-3-(2-methylpropyl)-5,7-dioxo-6-[(phenylmethyl)oxy]-2,3,5,7,11,11a-hexahydro[1,3]oxazolo-[3,2-*a*]pyrido[1,2-*d*]pyrazine-8-carboxamide (43 mg, 99%). This material was hydrogenated in a second step to give **47** (32 mg, 90%) as a white solid. ^{1}H NMR ($CDCl_3$) δ 11.47 (br, 1H), 10.29 (m, 1H), 8.35 (s, 1H), 7.39 (m, 1H), 6.80 (m, 2H), 5.31 (m, 1H), 4.62 (m, 2H), 4.44 (m, 2H), 4.37 (m, 1H), 3.88 (m, 1H), 3.84 (dd, J = 8.0, 5.6 Hz, 1H), 2.04 (m, 1H), 1.62 (m, 1H), 1.41 (m, 1H), 1.00 (d, J = 5.6 Hz, 3H), 0.99 (d, J = 6.0 Hz, 3H). ES$^+$ LC/MS: m/z calcd 447.16; found 448.15 (M + 1)$^+$.

(3*S*,11a*R*)-3-Butyl-*N*-[(2,4-difluorophenyl)methyl]-6-hydroxy-5,7-dioxo-2,3,5,7,11,11a-hexahydro[1,3]oxazolo[3,2-*a*]pyrido[1,2-*d*]pyrazine-8-carboxamide (48). 9b (40 mg, 0.09 mmol) and (2*S*)-2-amino-1-hexanol (100 mg) were reacted in dichloromethane (2 mL) with acetic acid to give (3*S*,11a*R*)-3-butyl-*N*-[(2,4-difluorophenyl)-methyl]-5,7-dioxo-6-[(phenylmethyl)oxy]-2,3,5,7,11,11a-hexahydro-[1,3]oxazolo[3,2-*a*]pyrido[1,2-*d*]pyrazine-8-carboxamide (43 mg, 94%). This material was hydrogenated in a second step to give **48** (33 mg, 92%) as a tinted white solid. ^{1}H NMR ($CDCl_3$) δ 11.48 (br, 1H), 10.27 (br, 1H), 8.36 (br, 1H), 7.31 (m, 1H), 6.77 (m, 2H), 5.28 (m, 1H), 4.59−4.36 (m, 5H), 3.83 (m, 2H), 2.08 (m, 1H), 1.58 (m, 1H), 1.39−1.23 (m, 4H), 0.90 (t, J = 6.8 Hz, 3H). ES$^+$ LC/MS: m/z calcd 447.16; found 448.06 (M + 1)$^+$.

(3*S*,11a*R*)-3-(Cyclohexylmethyl)-*N*-[(2,4-difluorophenyl)-methyl]-6-hydroxy-5,7-dioxo-2,3,5,7,11,11a-hexahydro[1,3]-oxazolo[3,2-*a*]pyrido[1,2-*d*]pyrazine-8-carboxamide (49). 9b (36 mg, 0.08 mmol) and (2*S*)-2-amino-3-cyclohexyl-1-propanol (30 mg, 0.19 mmol) were reacted in dichloromethane (2 mL) with acetic acid to give (3*S*,11a*R*)-3-(cyclohexylmethyl)-*N*-[(2,4-difluorophenyl)-methyl]-5,7-dioxo-6-[(phenylmethyl)oxy]-2,3,5,7,11,11a-hexahydro[1,3]-oxazolo[3,2-*a*]pyrido[1,2-*d*]pyrazine-8-carboxamide (27 mg, 61%). This material was hydrogenated in a second step to give **49** (25 mg, 99%) as a white solid. ^{1}H NMR ($CDCl_3$) δ 11.48 (br, 1H), 10.28 (s, 1H), 8.33 (s, 1H), 7.33 (m, 1H), 6.78 (m, 2H), 5.29 (m, 1H), 4.61 (m, 2H), 4.47−4.33 (m, 3H), 3.87−3.81 (m, 2H), 2.05 (m, 1H), 1.75−1.64 (m, 6H), 1.39 (m, 1H), 1.25−1.14 (m, 3H), 1.02−0.97 (m, 2H). ES$^+$ LC/MS: m/z calcd 487.19; found 488.35 (M + 1)$^+$.

(3*S*,11a*R*)-*N*-[(2,4-Difluorophenyl)methyl]-6-hydroxy-3-(hydroxymethyl)-5,7-dioxo-2,3,5,7,11,11a-hexahydro[1,3]-oxazolo[3,2-*a*]pyrido[1,2-*d*]pyrazine-8-carboxamide (50). 9b (50 mg, 0.10 mmol) and (2*R*)-2-amino-3-[(phenylmethyl)oxy]-1-propanol (0.1 mL) were reacted in dichloromethane (2 mL) with acetic acid to give (3*S*,11a*R*)-*N*-[(2,4-difluorophenyl)methyl]-5,7-dioxo-6-[(phenylmethyl)oxy]-3-{[(phenylmethyl)oxy]methyl}-2,3,5,7,11,11a-hexahydro[1,3]oxazolo[3,2-*a*]pyrido[1,2-*d*]pyrazine-8-carboxamide (61 mg, 99%). This material was hydrogenated in a second step to give **50** (37 mg, 87%) as a tinted white solid. ^{1}H NMR ($CDCl_3$/CD_3OD) δ 8.23 (s, 1H), 7.32 (m, 1H), 6.79 (m, 2H), 5.31 (d, J = 7.6 Hz, 1H), 4.56 (s, 2H), 4.42−4.36 (m, 3H), 4.17−4.11 (m, 2H), 3.85 (m, 1H), 3.62 (d, J = 11.2 Hz, 1H). ES$^+$ LC/MS: m/z calcd 421.11; found 422.07 (M + 1)$^+$.

(3*S*,11a*R*)-*N*-[(2,4-Difluorophenyl)methyl]-6-hydroxy-3-[2-(methylthio)ethyl]-5,7-dioxo-2,3,5,7,11,11a-hexahydro[1,3]-oxazolo[3,2-*a*]pyrido[1,2-*d*]pyrazine-8-carboxamide (51). 9b (43 mg, 0.09 mmol) and (2*S*)-2-amino-4-(methylthio)-1-butanol (0.1 mL) were reacted in 1,2-dichloroethane (5 mL) with acetic acid to give (3*S*,11a*R*)-*N*-[(2,4-difluorophenyl)methyl]-3-[2-(methylthio)ethyl]-5,7-dioxo-6-[(phenylmethyl)oxy]-2,3,5,7,11,11a-hexahydro[1,3]-oxazolo[3,2-*a*]pyrido[1,2-*d*]pyrazine-8-carboxamide (41 mg, 81%). This material (20 mg, 0.04 mmol) was treated with trifluoroacetic acid (1 mL) in dichloromethane (3 mL) at 0 °C to rt over 6 h. The mixture was concentrated in vacuo and subjected to reverse phase preparative HPLC purification to provide **51** (12 mg, 72%) as a white solid. ^{1}H NMR ($CDCl_3$) δ 11.35 (br, 1H), 10.25 (s, 1H), 8.34 (s, 1H), 7.33 (m, 1H), 6.79 (m, 2H), 5.32 (m, 1H), 4.62−4.53 (m, 3H), 4.43−4.39 (m, 2H), 3.91−3.87 (m, 2H), 2.63−2.53 (m, 2H), 2.39 (m, 1H), 2.12 (s, 3H), 1.89 (m, 1H). ES$^+$ LC/MS: m/z calcd 449.14; found 450.11 (M + 1)$^+$.

(3*S*,11a*R*)-*N*-[(2,4-Difluorophenyl)methyl]-6-hydroxy-3-[2-(methylsulfonyl)ethyl]-5,7-dioxo-2,3,5,7,11,11a-hexahydro-[1,3]oxazolo[3,2-*a*]pyrido[1,2-*d*]pyrazine-8-carboxamide (52). To a solution of (3*S*,11a*R*)-*N*-[(2,4-difluorophenyl)methyl]-3-[2-(methylthio)ethyl]-5,7-dioxo-6-[(phenylmethyl)oxy]-2,3,5,7,11,11a-hexahydro[1,3]oxazolo[3,2-*a*]pyrido[1,2-*d*]pyrazine-8-carboxamide (20 mg, 0.04 mmol) in dichloromethane (5 mL) at 0 °C was added *m*-CPBA (20 mg, 70%, 0.082 mmol). The resultant solution was allowed to warm as the bath warmed and stirred a total of 3 h. The reaction was quenched by the addition of $Na_2S_2O_3$ (aq) and sodium bicarbonate. The layers were separated and the organic layer washed with brine. The aqueous layer was extracted with dichloromethane and the combined organics dried over Na_2SO_4. Filtration and concentration provided (3*S*,11a*R*)-*N*-[(2,4-difluorophenyl)methyl]-3-[2-(methylsulfonyl)ethyl]-5,7-dioxo-6-[(phenylmethyl)oxy]-2,3,5,7,11,11a-hexahydro[1,3]oxazolo[3,2-*a*]pyrido[1,2-*d*]pyrazine-8-carboxamide (26 mg, 99%) as a white solid. This material was hydrogenated in a second step to give **52** (22 mg, 99%) as a white solid. ^{1}H NMR ($CDCl_3$) δ 11.00 (br, 1H), 10.16 (s, 1H), 8.33 (s, 1H), 7.36 (m, 1H), 6.81 (m, 2H), 5.42 (m, 1H), 4.62 (m, 3H), 4.41 (m, 2H), 3.93 (m, 2H), 3.31 (m, 2H), 2.98 (s, 3H), 2.40 (m, 1H), 2.28 (m, 1H). ES$^+$ LC/MS: m/z calcd 497.11; found 498.14 (M + 1)$^+$.

(3*S*,11a*R*)-*N*-[(2,4-Difluorophenyl)methyl]-6-hydroxy-5,7-dioxo-3-phenyl-2,3,5,7,11,11a-hexahydro[1,3]oxazolo[3,2-*a*]-pyrido[1,2-*d*]pyrazine-8-carboxamide (53). 9b (33 mg, 0.07 mmol) and L-phenylglycinol (19 mg, 0.14 mmol) were reacted in dichloromethane (2 mL) with acetic acid to give (3*S*,11a*R*)-*N*-[(4-fluorophenyl)methyl]-5,7-dioxo-3-phenyl-6-[(phenylmethyl)oxy]-2,3,5,7,11,11a-hexahydro[1,3]-oxazolo[3,2-*a*]pyrido[1,2-*d*]pyrazine-8-carboxamide (37 mg, 95%).

dx.doi.org/10.1021/jm400645w | J. Med. Chem. 2013, 56, 5901−5916

This material was hydrogenated in a second step to give **53** (33 mg, 99%) as a tinted white solid. ^{1}H NMR ($CDCl_3$) δ 11.23 (br, 1H), 10.27 (s, 1H), 8.39 (s, 1H), 7.43−7.32 (m, 6H), 6.80 (m, 2H), 5.58 (d, J = 6.8 Hz, 1H), 5.37 (apparent t, J = 6.8 Hz, 1H), 4.67−4.62 (m, 3H), 4.54 (d, J = 10.4 Hz, 1H), 4.11 (m, 1H), 4.01 (m, 1H). ES$^+$ LC/MS: m/z calcd 467.13; found 468.14 $(M + 1)^+$.

(3*S*,11a*R*)-*N*-[(2,4-Difluorophenyl)methyl]-6-hydroxy-5,7-dioxo-3-(phenylmethyl)-2,3,5,7,11,11a-hexahydro[1,3]-oxazolo[3,2-*a*]pyrido[1,2-*d*]pyrazine-8-carboxamide (54). **9b** (37 mg, 0.08 mmol) and (2*S*)-2-amino-3-phenyl-1-propanol (35 mg, 0.24 mmol) were reacted in dichloromethane (2 mL) with acetic acid to give (3*S*,11a*R*)-*N*-[(2,4-difluorophenyl)methyl]-5,7-dioxo-3-(phenylmethyl)-6-[(phenylmethyl)oxy]-2,3,5,7,11,11a-hexahydro[1,3]-oxazolo[3,2-*a*]pyrido[1,2-*d*]pyrazine-8-carboxamide (41 mg, 91%). This material was hydrogenated in a second step to give **54** (25 mg, 75%) as a white solid. ^{1}H NMR ($CDCl_3$) δ 11.47 (br, 1H), 10.28 (m, 1H), 8.35 (m, 1H), 7.37−7.26 (m, 4H), 7.18 (m, 2H), 6.79 (m, 2H), 5.03 (m, 1H), 4.64−4.61 (m, 3H), 4.40 (m, 1H), 4.23 (apparent t, J = 7.2 Hz, 1H), 3.96 (dd, J = 8.8, 6.4 Hz, 1H), 3.88 (apparent t, J = 11.2 Hz, 1H), 3.37 (dd, J = 13.6, 3.2 Hz, 1H), 2.99 (dd, J = 13.2, 8.8 Hz, 1H). ES$^+$ LC/MS: m/z calcd 481.14; found 482.14 $(M + 1)^+$.

(3*R*,11a*S*)-*N*-[(2,4-Difluorophenyl)methyl]-6-hydroxy-5,7-dioxo-3-(phenylmethyl)-2,3,5,7,11,11a-hexahydro[1,3]oxazolo[3,2-*a*]-pyrido[1,2-*d*]pyrazine-8-carboxamide (55). **9b** (34 mg, 0.07 mmol) and (2*R*)-2-amino-3-phenyl-1-propanol (D-phenylalaninol) (50 mg, 0.33 mmol) were reacted in dichloromethane (2 mL) with acetic acid to give (3*R*,11a*S*)-*N*-[(2,4-difluorophenyl)methyl]-5,7-dioxo-3-(phenylmethyl)-6-[(phenylmethyl)oxy]-2,3,5,7,11,11a-hexahydro[1,3]-oxazolo[3,2-*a*]pyrido[1,2-*d*]pyrazine-8-carboxamide (29 mg, 70%). This material was hydrogenated in a second step to give **55** (24 mg, 98%) as a white solid. ^{1}H NMR ($CDCl_3$) δ 11.46 (br, 1H), 10.27 (m, 1H), 8.33 (m, 1H), 7.32−7.16 (m, 6H), 6.78 (m, 2H), 5.02 (m, 1H), 4.61 (m, 3H), 4.39 (m, 1H), 4.22 (m, 1H), 3.95 (m, 1H), 3.87 (m, 1H), 3.36 (m, 1H), 2.97 (dd, J = 13.2 8.8 Hz, 1H). ES$^+$ LC/MS: m/z calcd 481.14; found 482.15 $(M + 1)^+$.

(3*S*,11a*R*)-*N*-[(2,4-Difluorophenyl)methyl]-6-hydroxy-3-[(4-hydroxyphenyl)methyl]-5,7-dioxo-2,3,5,7,11,11a-hexahydro-[1,3]oxazolo[3,2-*a*]pyrido[1,2-*d*]pyrazine-8-carboxamide (56). **9b** (40 mg, 0.09 mmol) and 4-[(2*S*)-2-amino-3-hydroxypropyl]phenol (43 mg, 0.21 mmol) were reacted in dichloromethane (2 mL) with acetic acid to give (3*S*,11a*R*)-*N*-[(2,4-difluorophenyl)methyl]-3-[(4-hydroxyphenyl)methyl]-5,7-dioxo-6-[(phenylmethyl)oxy]-2,3,5,7,11,11a-hexahydro[1,3]oxazolo[3,2-*a*]pyrido[1,2-*d*]pyrazine-8-carboxamide (10 mg, 20%). This material was hydrogenated in a second step to give **56** (7 mg, 63%) as a white solid. ^{1}H NMR (CD_3OD) δ 10.43 (m, 1H), 8.34 (s, 1H), 7.33 (m, 1H), 7.00 (d, J = 8.4 Hz, 2H), 6.82 (m, 2H), 6.71 (d, J = 8.4 Hz, 2H), 5.05 (m, 1H), 4.67−4.57 (m, 4H), 4.21 (dd, J = 8.8, 7.2 Hz, 1H), 3.94 (dd, J = 8.8, 6.4 Hz, 1H), 3.21 (dd, J = 13.2, 3.2 Hz, 1H), 2.90 (dd, J = 13.6, 8.8 Hz, 1H). ES$^+$ LC/MS: m/z calcd 497.14; found 498.18 $(M + 1)^+$.

(3*S*,11a*R*)-*N*-[(2,4-Difluorophenyl)methyl]-6-hydroxy-3-(1*H*-indol-3-ylmethyl)-5,7-dioxo-2,3,5,7,11,11a-hexahydro[1,3]-oxazolo[3,2-*a*]pyrido[1,2-*d*]pyrazine-8-carboxamide (57). **9b** (43 mg, 0.09 mmol) and (2*S*)-2-amino-3-(1*H*-indol-3-yl)-1-propanol (100 mg, 0.52 mmol) were reacted in 1,2-dichloroethane (5 mL) with acetic acid to give (3*S*,11a*R*)-*N*-[(2,4-difluorophenyl)methyl]-3-(1*H*-indol-3-ylmethyl)-5,7-dioxo-6-[(phenylmethyl)oxy]-2,3,5,7,11,11a-hexahydro[1,3]oxazolo[3,2-*a*]pyrido[1,2-*d*]pyrazine-8-carboxamide (36 mg, 64%). This material was hydrogenated in a second step to give (3*S*,11a*R*)-*N*-[(2,4-difluorophenyl)methyl]-6-hydroxy-3-(1*H*-indol-3-ylmethyl)-5,7-dioxo-2,3,5,7,11,11a-hexahydro[1,3]oxazolo[3,2-*a*]pyrido[1,2-*d*]pyrazine-8-carboxamide (29 mg, 95%) as a white solid. ^{1}H NMR ($CDCl_3$/CD_3OD) δ = 10.34 (m, 1H), 8.98 (br, 1H), 8.24 (s, 1H), 7.58 (d, J = 8.0 Hz, 1H), 7.32 (m, 2H), 7.15−7.01 (m, 3H), 6.78 (m, 2H), 4.94 (d, J = 6.8 Hz, 1H), 4.71 (d, J = 5.6 Hz, 1H), 4.59 (m, 2H), 4.35 (d, J = 10.4 Hz, 1H), 4.22 (m, 1H), 3.99 (m, 1H), 3.81 (m, 1H), 3.40 (dd, J = 13.6, 11.6 Hz, 1H), 3.18 (dd, J = 14.0, 8.4 Hz, 1H). ES$^+$ LC/MS: m/z calcd 520.16; found 521.18 $(M + 1)^+$.

Biological Methods. *Integrase Strand Transfer Assay.* Compounds were tested as inhibitors of recombinant HIV integrase in the following in vitro INST assay. A complex of integrase and biotinylated donor DNA−streptavidin-coated SPA beads was formed by incubating 2 μM recombinant integrase with 0.66 μM biotinylated donor DNA−4 mg/mL streptavidin-coated SPA beads in 25 mM sodium MOPS pH 7.2, 23 mM NaCl, 10 mM $MgCl_2$, 10 mM dithiothreitol, and 10% DMSO for 5 min at 37 °C. Beads were pelleted by centrifugation, supernatant removed, and the beads resuspended in 25 mM sodium MOPS pH 7.2, 23 mM NaCl, 10 mM $MgCl_2$. Beads were again spun down, supernatant removed, and the beads resuspended in a volume of 25 mM sodium MOPS pH 7.2, 23 mM NaCl, 10 mM $MgCl_2$ that would give 570 nM integrase (assuming all integrase bound the DNA beads). Test compounds dissolved and diluted in DMSO were added to the integrase−DNA complex to give 6.7% DMSO (typically 1 μL of compound added to 14 μL of integrase complex) and preincubated for 60 min at 37 °C. Then [3H] target DNA substrate was added to give a final concentration of 7 nM substrate, and the ST reaction was incubated at 37 °C typically for 25 to 45 min, which allowed for a linear increase in covalent attachment of the donor DNA to the radiolabeled target DNA. A 20 μL reaction was quenched by adding 60 μL of the following: 50 mM sodium EDTA, pH 8, 25 mM sodium MOPS, pH 7.2, 0.1 mg/mL salmon testes DNA, 500 mM NaCl. Streptavidin-coated SPA were from GE Healthcare, oligos to make the donor DNA were from Oligos Etc, and [3H] target DNA was a custom synthesis from Perkin-Elmer. Sequences of donor and target DNA were previously described (see ref 27) with the addition of seven terminal A's on each end of the target DNA that allowed for the incorporation of 14 tritiated T's (specific activity of target DNA approximately 1300 Ci/mmol).

pHIV Assay. VSV-G pseudotyped HIV vector expressing luciferase was generated by cotransfecting pGJ3-Luci (see ref 28) and pVSV-G (Clontech) into 293T cells by the calcium phosphate method. Approximately 5 h following transfection, the medium was exchanged. Sodium butyrate was added at 10 mM, and the cultures were incubated for approximately 40 h when the cell supernatants were harvested, filtered through a 0.45 or 1.0 μm filter, and stored at −80 °C. Compounds were dissolved in DMSO, diluted in medium (DMEM + 10% FCS), and plated at 100 μL per well in 96-well black, clear bottom tissue culture plates (Costar). 293T cells were harvested by trypsinization, counted, and mixed with PHIV viral vector in medium (DMEM + 10% FCS) . The amount of PHIV was adjusted to give approximately 100K CPM in the assay. Then 100 μL of cell−virus mixture was plated on top of the compounds to give 2×10^4 cells per well. The plates were incubated at 37 °C and 5% CO_2 for two days. The medium was aspirated from the plates, and 100 μL of prepared Steady Glo reagent (Promega) mixed 1:1 with medium was added per well. The plates were then read in a Topcount instrument (Perkin-Elmer) for 1 s per well. The effect of serum proteins on antiviral potency was evaluated with selected test compounds; in these instances, the standard assay was performed with the addition of 40 mg/mL HSA (catalogue no. A1653; Sigma, St. Louis, MO).

In Vivo Pharmacokinetic Methods. Male CD rats (n = 3), male beagle dogs (n = 2−4), and male cynomolgus monkeys (n = 2) received test article at doses of 1 mg/kg iv (1 mL/kg, formulated in a 20% *N*,*N*-dimethylacetamide/80% 0.05 M *N*-methylglucamine in 3% mannitol dosing vehicle for **3**, and in a 10% DMSO/10% Solutol/80% 0.05 M *N*-methylglucamine dosing vehicle for **4**) or 5 mg/kg po (2.5 mL/kg, suspended in a 0.5% methylcellulose aqueous solution or filled in a gelatin capsule). For fasted animals, the food supply was removed the evening before dosing and replaced at 4 h following dose administration; for all animals, water was provided ad libitum. Blood samples of rats, dogs, and monkeys were withdrawn from a surgically implanted venous cannula, a forelimb vein and a saphenous vein, respectively, at timed intervals for 24 h after dose administration, treated with EDTA, and centrifuged to harvest plasma for LC/MS/MS analysis. Plasma concentration−time data for individual rats were analyzed using noncompartmental analysis (WinNonlin v. 3.0A; Pharsight, Mountain View CA) to generate pharmacokinetic parameter estimates.

■ ASSOCIATED CONTENT

Supporting Information

Purity information, vibrational CD stereochemistry assignment data for **10R**, **10S**, **31**, and **32**, crystallographic data for **3**, HeLa cell fold-change values for Table 5, and additional synthetic details for the preparation of chiral amino-alcohols. This material is available free of charge via the Internet at http://pubs.acs.org

■ AUTHOR INFORMATION

Corresponding Author

*Phone: 919-483-6006. E-mail: brian.a.johns@gsk.com.

Author Contributions

B.A.J. and T.K. contributed equally to this manuscript.

Notes

The authors declare the following competing financial interest(s): BAJ is an employee of GlaxoSmithKline.

■ ACKNOWLEDGMENTS

This work was conducted and funded as part of a research collaboration between Shionogi & Co. Ltd. and GlaxoSmithKline. Dolutegravir and S/GSK744 are owned by Viiv Healthcare. We thank Douglas Minick for the VCD experiments, Pamela Golden for DMPK evaluations, Manon Villenevue and Eric Pullen for the SFC purifications, and Royston Copley for X-ray determination.

■ ABBREVIATIONS USED

HIV-1, human immunodeficiency virus type 1; ARV, antiretroviral; IN, integrase; INI, integrase inhibitor; INSTi, integrase strand transfer inhibitor; dsDNA, double-stranded DNA; BID, twice daily oral dosing; QD, once daily oral dosing; PK, pharmacokinetic; VCD, vibrational circlular dichroism spectroscopy; HS, human serum; HSA, human serum albumin; pHIV, pseudo HIV; PBMC, peripheral blood mononuclear cell; lbf, liver blood flow; MDCK, Madin−Darby canine kidney epithelial cells; P_{app}, apparent passive permeability; SFC, supercritical fluid chromatography; IPQC, immediate processing quality control; UPLC, ultra performance liquid chromatography

■ REFERENCES

(1) *UNAIDS Report on the Global AIDS Epidemic*; United Nations Program on HIV/AIDS (UNAIDS): Geneva, December, 2012; www.UNAIDS.org.

(2) (a) Pendri, A.; Meanwell, N. A.; Peese, K. M.; Walker, M. A. New first and second generation inhibitors of human immunodeficiency virus-1 integrase. *Expert Opin. Ther. Pat.* **2011**, *21*, 1173−1189. (b) Johns, B. A.; Svolto, A. C. Advances in two-metal chelation inhibitors of HIV integrase. *Expert Opin. Ther. Pat.* **2008**, *18*, 1225−1237. (c) Kawasuji, T.; Yoshinaga, T.; Sato, A.; Yodo, M.; Fujiwara, T.; Kiyama, R. A platform for designing HIV integrase inhibitors. Part 1. 2-Hydroxy-3-heteroaryl acrylic acid derivatives as novel HIV integrase inhibitors and modeling of hydrophilic and hydrophobic pharmacophores. *Bioorg. Med. Chem.* **2006**, *14*, 8430−8445. (d) Kawasuji, T.; Fuji, M.; Yoshinaga, T.; Sato, A.; Fujiwara, T.; Kiyama, R. A platform for designing HIV integrase inhibitors. Part 2: A two-metal binding model as a potential mechanism of HIV integrase inhibitors. *Bioorg. Med. Chem.* **2006**, *14*, 8420−8429.

(3) Lennox, J. L.; DeJesus, E.; Lazzarin, A.; Pollard, R. B.; Madruga, J. V. R.; Berger, D. S.; Zhao, J.; Xu, X.; Williams-Diaz, A.; Rodgers, A. J.; Barnard, R. J. O.; Miller, M. D.; DiNubile, M. J.; Nguyen, B.-Y.; Leavitt, R.; Sklar, P. Safety and efficacy of raltegravir-based versus efavirenz-based combination therapy in treatment-naive patients with HIV-1 infection: a multicentre, double-blind randomised controlled trial. *Lancet* **2009**, *374*, 796−806.

(4) Ceccherini-Silberstein, F.; Malet, I.; D'Arrigo, R.; Antinori, A.; Marcelin, A.-G.; Perno, C-F Characterization and structural analysis of HIV-1 integrase conservation. *AIDS Rev.* **2009**, *11*, 17−29.

(5) Johnson, V. A.; Brun-Vezinet, F.; Clotet, B.; Gunthard, H. F.; Kuritkes, D. R.; Pillay, D.; Schapiro, J. M.; Richman, D. D. Update of the Drug Resistance Mutations in HIV-1. *Top. HIV Med.* **2010**, *18*, 156−163.

(6) (a) Quashie, P. K.; Sloan, R. D.; Wainberg, M. A. Novel therapeutic strategies targeting HIV integrase. *BMC Med.* **2012**, *10*, 34. (b) Goethals, O.; Clayton, R.; Van Ginderen, M.; Vereycken, I.; Wagemans, E.; Geluykens, P.; Dockx, K.; Strijbos, R.; Smits, V.; Vos, A.l; Meersseman, G.; Jochmans, D.; Vermeire, K.; Schols, D.; Hallenberger, S.; Hertogs, K. Resistance mutations in human immunodeficiency virus type 1 integrase selected with elvitegravir confer reduced susceptibility to a wide range of integrase inhibitors. *J. Virol.* **2008**, *82*, 10366−10374.

(7) Ramanathan, S.; Mathias, A. A.; German, P.; Kearney, B. P. Clinical pharmacokinetic and pharmacodynamic profile of the HIV integrase inhibitor elvitegravir. *Clin. Pharmacokinet.* **2011**, *50*, 229−244.

(8) Blanco, J.-L.; Varghese, C.; Rhee, S.-Y.; Gatell, J. M.; Shafer, R. W. HIV-1 Integrase Inhibitor Resistance and Its Clinical Implications. *J. Infect. Dis.* **2011**, *203*, 1204−1214.

(9) Kawasuji, T.; Johns, B. A.; Yoshida, H.; Taishi, T.; Taoda, Y.; Murai, H.; Kiyama, R.; Fuji, M.; Yoshinaga, T.; Seki, T.; Kobayashi, M.; Sato, A.; Fujiwara, T. Carbamoyl pyridone HIV-1 integrase inhibitors. 1. Molecular design and establishment of an advanced two-metal binding pharmacophore. *J. Med. Chem.* **2012**, *55*, 8735−8744.

(10) Kawasuji, T.; Johns, B. A.; Yoshida, H.; Weatherhead, J. G.; Akiyama, T.; Taishi, T.; Taoda, Y.; Mikamiyama-Iwata, M.; Murai, H.; Kiyama, R.; Fuji, M.; Yoshinaga, T.; Seki, T.; Kobayashi, M.; Sato, A.; Garvey, E. P.; Fujiwara, T. Carbamoyl Pyridone HIV-1 Integrase Inhibitors 2. Bi- and Tricyclic Derivatives Result in Superior Antiviral and Pharmacokinetic Profiles. *J. Med. Chem.* **2013**, *56*, 1124−1135.

(11) Johns, B. A.; Kawasuji, T.; Taishi, T.; Taoda, Y.; Polycyclic carbamoylpyridone derivative having HIV integrase inhibitory activity. WO 2006/116764 A1, 2006.

(12) Agrawal, A.; DeSoto, J.; Fullagar, J. L.; Maddali, K.; Rostami, S.; Richman, D. D.; Pommier, Y.; Cohen, S. M. Probing chelation motifs in HIV integrase inhibitors. *Proc. Natl. Acad. Sci. U. S. A.* **2012**, *109*, 2251.

(13) For additional discussion on inhibitors viral enzymes through metal chelating mechanisms, see (a) Kirschberg, T.; Parrish, J. Metal chelators as antiviral agents. *Curr. Opin. Drug Discovery Dev.* **2007**, *10*, 460. (b) Rogolino, D.; Carcelli, M.; Sechi, M.; Neamati, N. *Coord. Chem. Rev.* **2012**, *256*, 3063.

(14) Pseudo-type HIV assay (PHIV). Garvey, E. P.; Johns, B. A.; Gartland, M. J.; Foster, S. A.; Miller, W. H.; Ferris, R. G.; Hazen, R. J.; Underwood, M. R.; Boros, E. E.; Thompson, J. B.; Weatherhead, J. G.; Koble, C. S.; Allen, S. H.; Schaller, L. T.; Sherrill, R. G.; Yoshinaga, T.; Kobayashi, M.; Wakasa-Morimoto, C.; Miki, S.; Nakahara, K.; Noshi, T.; Sato, A.; Fujiwara, T. The naphthyridinone GSK364735 is a novel, potent human immunodeficiency virus type 1 integrase inhibitor and antiretroviral. *Antimicrob. Agents Chemother.* **2008**, *52*, 901−908.

(15) Data for *rac*-**8** and its isomers against the Q148K site directed mutant were obtained using HeLa CD4 β-gal assay. Subsequent data presented herein was obtained using the pseudo-HIV assay system unless noted otherwise.

(16) Minick, D. J.; Rutkowske, R. D.; Miller, L. A. D. Strategies for Successfully Applying Vibrational Circular Dichroism Spectroscopy. *Am. Pharm. Rev.* **2007**, *10*, 118−123.

(17) Kawasuji, T.; Johns, B. A.; Yoshida, H.; Taoda, Y.; Akiyama, T.; Taishi, T.; Kiyama, R.; Fuji, M.; Murai, H.; Yoshinaga, T.; Sato, A.; Fujiwara, T. The Design of Carbamoyl Puyridone Integrase Inhibitors and Discovery of Dolutegravir (S/GSK1349572). 244th American Chemical Society National Meeting, Philadelphia, PA, August 19−23, 2012, MEDI-357.

(18) The fold change in antiviral IC_{50} for raltegravir against the Q148K site directed mutant is consistent with values observed in related assay systems in ref 17. Also see (a) Canducci, F.; Marinozzi, M. C.; Sampaolo, M.; Boeri, E.; Spagnuolo, V.; Gianotti, N.; Castagna, A.; Paolucci, S.; Baldanti, F.; Lazzarin, A.; Clementi, M. Genotypic/phenotypic patterns

of HIV-1 integrase resistance to raltegravir. *J. Antimicrob. Chemother.* **2010**, *65*, 425−433. (b) Goethals, O.; Vos, A.; Van Ginderen, M.; Geluykens, P.; Smits, V.; Schols, D.; Hertogs, K.; Clayton, R. Primary mutations selected in vitro with raltegravir confer large fold changes in susceptibility to first-generation integrase inhibitors, but minor fold changes to inhibitors with second-generation resistance profiles. *Virology* **2010**, *402*, 338−346.

(19) C24/$^{pHIV}PAIC_{90}$ ratios were determined using C24h concentrations of 908 ng/mL for **3** and 9592 ng/mL for **4**. $^{pHIV}PAIC_{90}$ values were determined estimated using four times the $^{pHIV}PAIC_{50}$ values to give estimates of 37.4 ng/mL for **3** and 49.1 ng/mL for **4**.

(20) Kobayashi, M.; Yoshinaga, T.; Seki, T.; Wakasa-Morimoto, C.; Brown, K. W.; Ferris, R.; Foster, S. A.; Hazen, R. J.; Miki, S.; Suyama-Kagitani, A.; Kawauchi-Miki, S.; Taishi, T.; Kawasuji, T.; Johns, B. A.; Underwood, M. R.; Garvey, E. P.; Sato, A.; Fujiwara, T. In vitro antiretroviral properties of S/GSK1349572, a next-generation HIV integrase inhibitor. *Antimicrob. Agents Chemother.* **2011**, *55*, 813.

(21) Yoshinaga, T.; Kobayashi, M.; Seki, T.; Kawasuji, T.; Taishi, T.; Sato, A.; Fujiwara, T.; Johns, B.; Hazen, R.; Ferris, R.; Underwood, M. Antiviral Characteristics of S/GSK1265744, an HIV integrase inhibitor dosed by oral or long-acting parenteral injection. 52nd Interscience Conference on Antimicrobial Agents and Chemotherapy (ICAAC), San Francisco, CA, September 9−12, 2012, H-550.

(22) (a) Krishnan, L.; Naraharisetty, H. L.; Hare, S.; Cherepanov, P.; Engelman, A. Structure-based modeling of the functional HIV-1 intasome and its inhibition. *Proc. Natl. Acad. Sci. U. S. A.* **2010**, *107*, 15910. (b) Hare, S.; Vos, A. M.; Clayton, R. F.; Thuring, J. W.; Cummings, M. D.; Cherepanov, P. Molecular mechanisms of retroviral integrase inhibition and the evolution of viral resistance. *Proc. Natl. Acad. Sci. U. S. A.* **2010**, *107*, 20057. (c) Hare, S.; Smith, S. J.; Métifiot, M.; Jaxa-Chamiec, A.; Pommier, Y.; Hughes, S. H.; Cherepanov, P. Structural and functional analyses of the second-generation integrase strand transfer inhibitor dolutegravir (S/GSK1349572). *Mol. Pharmacol.* **2011**, *80*, 565.

(23) Liver blood flow values used (mL/min/kg) were 55 (rat), 31 (dog), and 44(monkey) according to Davies, B.; Morris, T. Physiological parameters in laboratory animals and humans. *Pharm. Res.* **1993**, *10*, 1093.

(24) For reports on the clinical trial evaluation of S/GSK572, see (a) Min, S.; Song, I.; Borland, J.; Chen, S.; Lou, Y.; Fujiwara, T.; Piscitelli, S. Pharmacokinetics and safety of S/GSK1349572, a next-generation HIV integrase inhibitor, in healthy volunteers. *Antimicrob. Agents Chemother.* **2010**, *54*, 254−258. (b) Min, S.; Sloan, L.; DeJesus, E.; Hawkins, T.; McCurdy, L.; Song, I.; Stroder, R.; Chen, S.; Underwood, M.; Fujiwara, T.; Piscitelli, S.; Lalezari, J. Antiviral activity, safety, and pharmacokinetics/pharmacodynamics of dolutegravir as 10-day monotherapy in HIV-1-infected adults. *AIDS (Hagerstown, MD, U. S.)* **2011**, *25*, 1737−1745. (c) Lunzen, J. v.; Maggiolo, J. R.; Rakhmanova, A.; Yeni, P.; Young, B.; Rockstroh, J. K.; Almond, S.; Song, I.; Brothers, C.; Min, S. Once daily dolutegravir (S/GSK1349572) in combination therapy in antiretroviral-naive adults with HIV: planned interim 48 week results from SPRING-1, a dose-ranging, randomised, phase 2b trial. *Lancet Infect. Dis.* **2012**, *12*, 111−118. (d) Raffi, F.; Rachlis, A.; Stellbrink, H. −J.; Hardy, W. D.; Torti, C.; Orkin, C.; Bloch, M.; Podzamczer, D.; Pokrovsky, V.; Pulido, F.; Almond, S.; Margolis, D.; Brennan, C.; Min, S. Once-daily dolutegravir versus raltegravir in antiretroviral-naive adults with HIV-1 infection: 48 week results from the randomised, double-blind, non-inferiority SPRING-2 study. *Lancet* **2013**, in press. (e) Walmsley, S.; Antela, A.; Clumeck, N.;Duiculescu, D.; Eberhard, A.; Gutiérrez, F.; Hocqueloux, L.; Maggiolo, F.; Sandkovsky, U.; Granier, C.; Wynne, B.; Pappa, K. Dolutegravir (DTG; S/GSK1349572) + Abacavir/Lamivudine Once Daily Statistically Superior to Tenofovir/Emtricitabine/Efavirenz: 48-Week Results—SINGLE (ING114467). 52nd Interscience Conference on Antimicrobials and Chemotherapy (ICAAC), San Francisco, CA, September 9−12, 2012, H-556b.

(25) Min, S.; DeJesus, E.; McCurdy, L.; Richmond, G.; Torres, J.; Ford, S.; Chen, S.; Lou, Y.; Bomar, M.; Cyr, T.; St.Clair, M.; Fujiwara, T.; Piscitelli, S. Pharmacokinetics (PK) and Safety in Healthy and HIV-Infected Subjects and Short-Term Antiviral Efficacy of S/GSK1265744, a Next Generation Once Daily HIV Integrase Inhibitor. 49th Interscience Conference on Antimicrobial Agents and Chemotherapy (ICAAC), San Francisco, CA, September 12−15, 2009, H-1228.

(26) Spreen, W.; Ford, S. L.; Chen, S.; Gould, E.; Wilfret, D.; Subich, D.; Taishi, T.; Hong, Z. Pharmacokinetics, Safety and Tolerability of the HIV Integrase Inhibitor S/GSK1265744 Long Acting Parenteral Nanosuspension Following Single Dose Administration to Healthy Adults. XIX International AIDS Conference, Washington DC, July 22−27, 2012, TUPE040.

(27) Hazuda, D. J.; Hastings, J. C.; Wolfe, A. L.; Emini, E. A. A novel assay for the DNA strand-transfer reaction of HIV-1 integrase. *Nucleic Acids Res.* **1994**, *22*, 1121−1122.

(28) Jarmy, G.; Heinkelein, M.; Weissbrich, B.; Jassoy, C.; Rethwilm, A. Phenotypic analysis of the sensitivity of HIV-1 to inhibitors of the reverse transcriptase, protease, and integrase using a self-inactivating virus vector system. *J. Med. Virol.* **2001**, *64*, 223−231.